

PHYTOCHROME-INTERACTING FACTOR 7 and RELATIVE OF EARLY FLOWERING 6 act in shade avoidance memory in *Arabidopsis*

Received: 25 October 2023

Qican Cheng¹, Yue Zeng¹, Sha Huang¹, Chuanwei Yang², Yu Xie¹, Wen-Hui Shen³ & Lin Li¹✉

Accepted: 8 August 2024

Published online: 13 September 2024

 Check for updates

Shade avoidance helps plants maximize their access to light for growth under crowding. It is unknown, however, whether a priming shade avoidance mechanism exists that allows plants to respond more effectively to successive shade conditions. Here, we show that the shade-intolerant plant *Arabidopsis* can remember a first experienced shade event and respond more efficiently to the next event on hypocotyl elongation. The transcriptional regulator PHYTOCHROME-INTERACTING FACTOR 7 (PIF7) and the histone H3K27-demethylase RELATIVE OF EARLY FLOWERING 6 (REF6) are identified as being required for this shade avoidance memory. RNA-sequencing analysis reveals that shade induction of shade-memory-related genes is impaired in the *pif7* and *ref6* mutants. Based on the analyses of enrichments of H3K27me3, REF6 and PIF7, we find that priming shade treatment induces PIF7 accumulation, which further recruits REF6 to demethylate H3K27me3 on the chromatin of certain shade-memory-related genes, leading to a state poised for their transcription. Upon a second shade treatment, enhanced shade-mediated inductions of these genes result in stronger hypocotyl growth responses. We conclude that the transcriptional memory mediated by epigenetic modification plays a key role in the ability of primed plants to remember previously experienced shade and acquire enhanced responses to recurring shade conditions.

Plant growth and crop production are strongly affected by environmental conditions. Plants can detect the proximity of other plants by perceiving a change in the ratio of red light to far-red (R/FR) light from neighbouring plants and trigger a series of changes in architecture and physiology; this phenomenon is called shade avoidance syndrome (SAS)¹. The phenotypes associated with SAS include increased elongation of internodes and/or petioles, reduced leaf growth, and increased apical dominance, which occur together as an attempt of plants to avoid being shaded². Prolonged exposure to shade evokes the acceleration of flowering³, seed set reduction, and susceptibility to herbivores^{2,4}.

In recent years, the molecular mechanisms underlying shade-avoidance responses have been elucidated, mostly through studies in *Arabidopsis*. A reduction in R/FR irradiance is perceived by phytochromes (e.g., phyB)⁵. Typically, a phytochrome molecule exists in one of the two conformations, Pr and Pfr, the latter being the active form. The absorption of R light converts Pr to Pfr, whereas FR absorption reverts Pfr to Pr. PHYTOCHROME-INTERACTION FACTORs (PIFs) are basic HLH transcription factors capable of promoting stem extension growth⁶. PIF7 is considered a master regulator of SAS, as evidenced by the strong shade-defective response of *pif7* mutant plants^{7,8}. PIF7 is less

¹State Key Laboratory of Genetic Engineering, Institute of Plants Biology, School of Life Sciences, Fudan University, Shanghai, People's Republic of China.

²Ministry of Education Key Laboratory for Biodiversity Science and Ecological Engineering, Institute of Biodiversity Science, School of Life Sciences, Fudan University, Shanghai, China. ³Institut de Biologie Moléculaire des Plantes, CNRS, Université de Strasbourg, Strasbourg, France. ✉e-mail: linli@fudan.edu.cn

vulnerable than PIF1/3/4/5 to the rapid turnover induced by the Pfr form of phyB. The activity of PIF7 is controlled by rapid dephosphorylation in response to shade^{8,9}. Due to the reversible interconversion between the two states of phytochromes according to the R/FR ratio, the effects of shade on downstream gene expression and the organ elongation growth rate are reversible^{10,11}. For example, the abundance of the *PHYTOCHROME-INTERACTING FACTOR 3-LIKE 1* (*PIF1*) transcript increased 35-fold after 1 h of exposure to a low R/FR ratio and quickly decreased after a return to a high R/FR ratio¹². Accordingly, the growth rate of hypocotyls increases under low R/FR treatment and decreases after reversion to high R/FR¹⁰.

More recent studies have revealed that some chromatin modifiers are involved in SAS. It has been shown that PIF7 interacts with MRG1/MRG2, which recruits histone acetylases to perform histone acetylation and promote the expression of shade-responsive genes¹³. HDA9 cooperates with PIF4/7 to regulate shade/auxin-responsive genes in response to shade¹⁴. PIFs also act in modifying the epigenetic landscape of the histone variants H2A.Z and H3.3 via interactions with EIN6 ENHANCER (EEN) and ANTI-SILENCING FACTOR 1 (ASF1) in response to shade^{9,15}. Shade also induces the production of lncRNAs (long non-coding RNAs) involved in modulating SAS¹⁶.

While molecular memory mechanisms are involved in plant adaptation to diverse biotic and abiotic stresses¹⁷, thus far, it is unknown whether plants can remember the first experienced shade and change their growth strategy in response to the second shade exposure. Thus, our study aimed to explore the memory of the shade avoidance response of *Arabidopsis* seedlings. We found that

Arabidopsis seedlings can remember 8 h of primed shade after 40 h recovery, triggering faster hypocotyl elongation when exposed to shade again. Based on the phenotypic responses of several examined *Arabidopsis* mutants, *ref6* and *pi7* were found to abolish shade memory. RELATIVE OF EARLY FLOWERING 6 (REF6, also known as JM12) is required for normal shade-induced hypocotyl elongation and is responsible for demethylating H3K27me3 on REF6-targeted shade-induced genes. During the priming shade, PIF7 physically interacts with REF6, which demethylates H3K27me3 on certain PIF7-targeted shade-induced genes. Although these genes return to lower levels of expression during the recovery stage, they are maintained in a poised state, making them ready for induction, which results in stronger shade induction when shade occurs again.

Results

Arabidopsis seedlings exhibit shade avoidance memory

Using the DynaPlant system¹⁸, we monitored the time-lapse growth rates of hypocotyl elongation of *Arabidopsis* seedlings during white light/shade transitions. We found that shade-induced high growth rates gradually decreased to low levels over approximately 8–9 h after the Col-0 seedlings being transferred to white light (Fig. 1a). To test whether plants can remember their first experienced shade (priming with 2/4/8/10 h of shade), we exposed them to a second shade (triggering) after 40 h of white light recovery (recovering), which allowed their growth rate to return completely to the baseline level before triggering. As shown in Fig. 1b, c, the growth rates in response to triggering shade were similar between naïve (N, not exposed to a

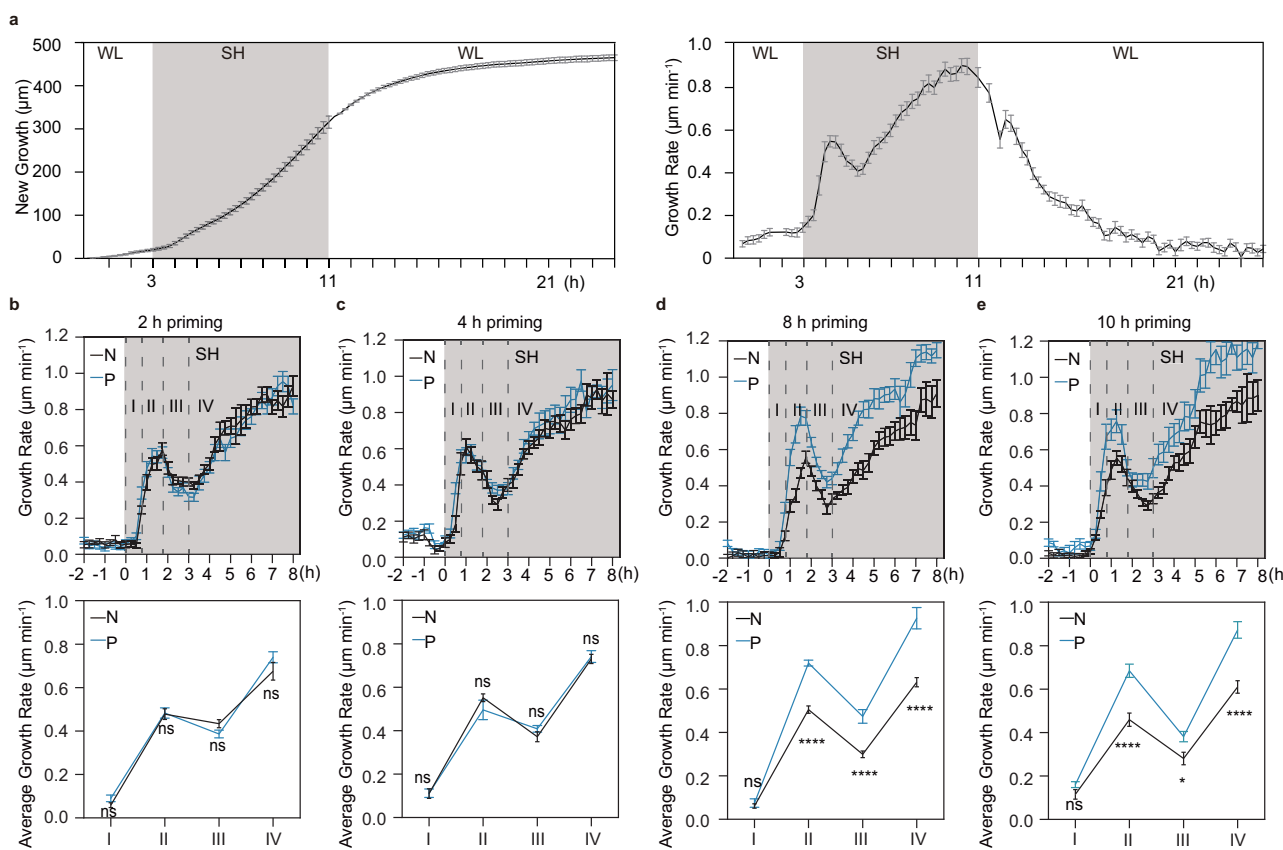


Fig. 1 | *Arabidopsis* seedlings exhibit a shade avoidance memory in indicated light condition. **a** New growth and growth rates and of 6-day-old Col-0 seedlings treated with shade (SH) white light (WL). New growth and real-time growth rate were recorded at 15-min intervals. Shade triggered growth rates of Col-0 seedlings grown under naïve (N) and 2 (b), 4 (c), 8 (d) or 10 (e) h shade-primed (P) conditions. The top panel is real-time growth rates recorded at 15-min intervals for 8 h captured

by DynaPlant system. The bottom panel is average growth rates calculated from new growth in four-time spans: I (0–0.75 h), II (0.75–1.75 h), III (1.75–3 h), IV (3–8 h). Data are presented as mean values \pm SEM. Student's two-sided *t*-test was used to calculate the *P* value between the indicated spans, and significant differences are shown by *(*P* < 0.05), **(*P* < 0.001) and ***(*P* < 0.0001) and ns (*P* > 0.05). Source data are provided as a Source Data file.

priming shade) and 2 or 4 h shade-primed (P) seedlings. However, 8/10 h shade-primed seedlings grew significantly faster than naïve plants during triggering shade (Fig. 1d, e).

We also measured the final hypocotyl lengths of naïve and primed seedlings after 48 h of triggering shade. Consistent with the growth rates, 8/10 h but not 2/4 h shade-primed seedlings showed longer hypocotyls than naïve plants (Supplementary Fig. 1a). This difference in hypocotyl length could have been caused by the priming shade induced elongation and/or a faster growth during the triggering shade caused by the memory of the priming shade. We found that the hypocotyl grew approximately 300 μ m after the 8 h of priming shade, which was much less than the difference between naïve and primed seedlings after triggering shade treatment, indicating that plants remember the priming shade to accelerate growth when exposed to shade again.

To test the effects of recovery duration on the memory of the 8 h of shade priming, we extended the recovery time from 40 h to 48 h or 72 h. As shown in Supplementary Fig. 1b, the difference between naïve and shade-primed seedlings decreased with increasing recovery time. The faster growth caused by the memory of 8 h priming shade was detectable after 24 h and 48 h triggering shade application (Supplementary Fig. 1c).

Taken together, the results showed that *Arabidopsis* seedlings could remember the experience of 8 h priming shade, leading to faster growth after 40 h of recover when the second triggering shade occurred. The treatment of seedlings shown in Supplementary Fig. 1d was applied to detected final hypocotyl length of shade avoidance memory (P growth condition).

To provide further evidence for bona fide shade avoidance memory, we investigated the shade memory phenotypes of *pif7-1* and several histone modification mutants, including *ref6-1* and *ref6-3* (two allelic mutants of *REF6/JMJ12*, encoding H3K27me3 demethylase), *elf6-*

3 (a mutant of *ELF6/JMJ11*, encoding H3K27me3 demethylase), *jmj13g* (a mutant of *JMJ13*, encoding H3K27me3 demethylase), *ref6-1elf6-3*, *clf28* (a mutant of *CLF*, encoding H3K27me3 methyltransferase), *atx1-2* (a mutant of *ATX*, encoding H3K4me3 methyltransferase), *sdg25-1* (a mutant of *SDG25*, encoding H3K4me3 methyltransferase), *sdg8* (a mutant of *SDG8*, encoding H3K36me3 methyltransferase), and *atx1-2sdg25-1*. The hypocotyl lengths of *jmj13g*, *clf28*, *atx1-2*, *sdg25-1*, *sdg8*, *atx1-2sdg25-1* and *proREF6::REF6-HA/ref6-1* were similar with the wild-type control Col-0 grown under P condition (Supplementary Fig. 1d–e). However, the hypocotyl lengths of shade avoidance memory were markedly decreased in *pif7-1*, *ref6-1*, *ref6-3*, *elf6-3*, and *ref6-1elf6-3* (Supplementary Fig. 1e), indicating that shade avoidance memory is indeed gene function dependent.

PIF7 and REF6 are required for shade avoidance memory and the shade avoidance response

Among the mutants we screened for shade avoidance memory (Supplementary Fig. 1e), growth rate measurements also confirmed that the *ref6-1*, *ref6-3*, *elf6-3*, *ref6-1elf6-3* and *pif7-1* mutants but not the *proREF6::REF6-HA/ref6-1*, *sdg25-1atx1-2*, *sdg25-1*, *atx1-2* and *jmj13g* mutants, displayed growth defects in phase II and phase IV under shade-primed (P) condition (Fig. 2a, Supplementary Fig. 2a). ELF6 and JMJ13 are close homologues of REF6. Mutant of *ELF6* displayed a defective shade memory phenotype, while the mutant of *JMJ13* did not. The growth defect in the shade memory phenotype was stronger in the double mutant *ref6-1elf6-3* than that in any of the two single mutants, indicating the functional redundancy between *REF6* and *ELF6* in terms of shade memory. These results suggest that PIF7 and REF6/ELF6 are required for shade avoidance memory. We also monitored the growth rates of *ref6-1*, *proREF6::REF6-HA/ref6-1*, *ref6-3*, *elf6-3*, *ref6-1elf6-3* and *pif7-1* under naïve (N) condition. Unlike the growth rates under P condition, the shade growth defects of *ref6-1*, *ref6-3*, *elf6-3*, and *ref6-*

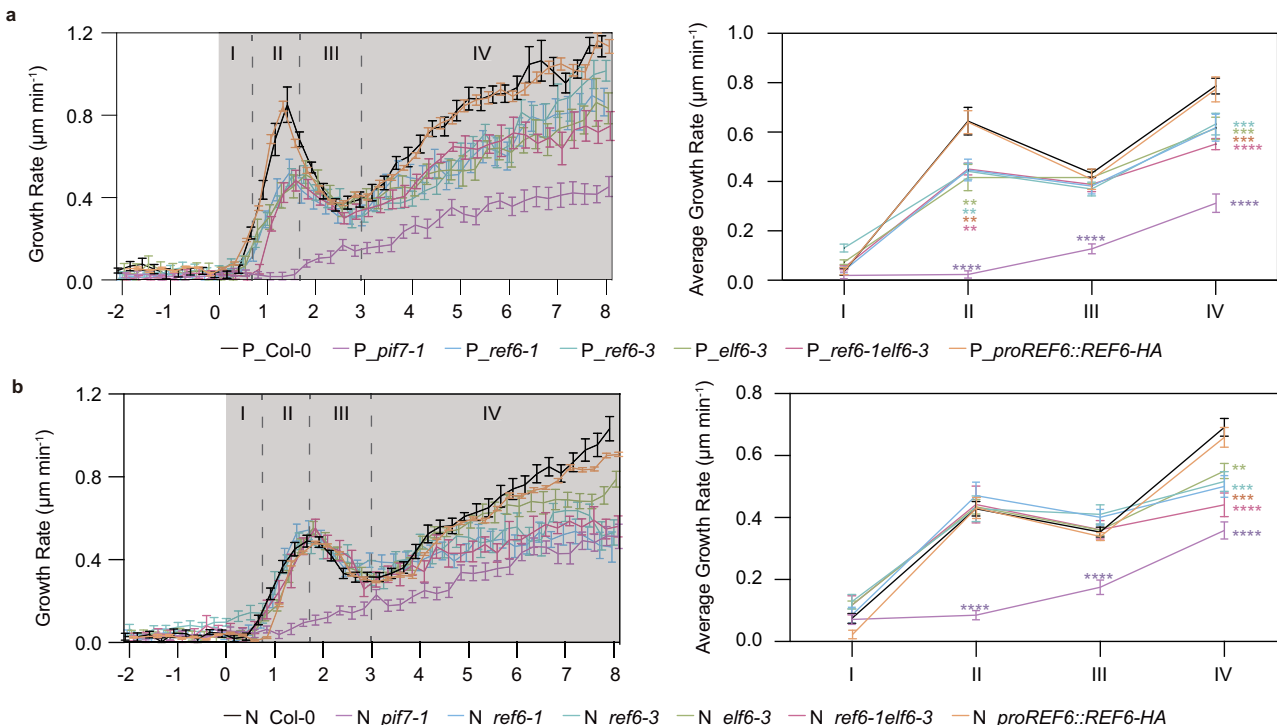


Fig. 2 | PIF7 and REF6 are required for shade avoidance memory and shade avoidance response. Shade-triggered growth rates and average growth rates of Col-0, *ref6-1*, *proREF6::REF6-HA/ref6-1*, *ref6-3*, *elf6-3*, *ref6-1elf6-3* and *pif7-1* seedlings grown under P (a) and N (b) conditions. The left panel shows real-time growth rates calculated from new growth which was captured by DynaPlant system. The right

panel is average growth rates in four time spans. Data are presented as mean values \pm SEM. Student's two-sided *t*-test was used to calculate the *P* value between the indicated genotypes, and significant differences are shown by **(*P* < 0.01), ***(*P* < 0.001) and ****(*P* < 0.0001). Source data are provided as a Source Data file.

elf6-3 under N condition mainly occurred in phase IV but not phase II (Fig. 2b), indicating a possible difference in the mechanisms involved between the N and P conditions.

To check the growth rate in more detail, we measured the kinetics of growth decay after the priming shade treatment in Col-0, *pif7-1*, *ref6-1* and *ref6-3* mutants (Supplementary Fig. 2b, c). The mean time for extension growth to return to the level before shade treatment was approximately 8–9 h in Col-0, 4–5 h in *ref6-3/ref6-1*, and 3–4 h in *pif7-1*, suggesting that PIF7 and REF6 mediate the persistent effects of 8 h shade on hypocotyl elongation.

To further address the role of *REF6/ELF6* in shade avoidance under N condition, 3-day-old seedlings grown under white light were transferred to shade for 4 d as normal conditions for the detection of shade-induced hypocotyl elongation. We found that *ref6-1*, *ref6-3*, *elf6-3*, and *ref6-1elf6-3* exhibited markedly attenuated responses to shade compared with Col-0 (Supplementary Fig. 2d). The attenuated hypocotyl length of the *ref6-1* mutant could be rescued by *proREF6:REF6-HA* complementation (Supplementary Fig. 2d). In contrast, the seedlings of *sdg25-1atx1-2*, *sdg25-1*, *atx1-2* and *jmj13g* displayed the similar shade-induced hypocotyl elongation with Col-0, indicating that these genes may play no role on shade response and shade memory (Supplementary Fig. 2d).

To investigate the genetic relationships between *REF6/ELF6* and *PIF7/phyB*, we generated *ref6-1pif7-1*, *ref6-3pif7-1*, *elf6-3pif7-1*, *ref6-1phyB-9*, and *elf6-3phyB-9*. Under N conditions, the hypocotyl lengths of *ref6-1pif7-1*, *ref6-3pif7-1* and *elf6-3pif7-1* were closer to that of *pif7-1* (Supplementary Fig. 2d). Under white light conditions, loss of function of *REF6/ELF6* could partially repress the long-hypocotyl phenotype of *phyB-9* (Supplementary Fig. 2e), indicating that *REF6* functions downstream of *phyB*. These results suggest that *REF6* and *ELF6* are involved in *phyB-PIF7*-modulated shade-induced hypocotyl elongation.

REF6 demethylates H3K27me3 on late shade-induced genes

Given the finding that the growth defects of *ref6-1* and *ref6-3* occur relatively late (phase IV) under N conditions, we wondered whether *REF6* differentially regulates early and late shade-responsive genes. Exploiting a previously published RNA-sequencing dataset (GSE59722) that includes data profiles of both 1 h and 7 h shade treatments, we first reanalysed the differentially expressed genes (DEGs) with cut-off $FC > 2$ and $FDR < 0.05$, and we identified 1 h shade-induced genes (162) and 7 h shade-induced genes (739) (Fig. 3a, Supplementary Data 1). We then searched for their overlaps with genes bound by *REF6* (2836 genes, GSE65329¹⁹). A higher number of *REF6*-bound genes were found overlapped with 7 h than 1 h shade-induced genes (Fig. 3a, Supplementary Data 2). These genes were enriched in growth related Gene Ontology (GO) categories, including hormone-mediated signalling pathway, developmental growth and cell wall biogenesis or organization (Fig. 3b, Supplementary Data 3).

Moreover, in Col-0 grown under white light, the 7 h shade-induced genes displayed a drastically lower basal-level of H3K27me3 than the control reference genes (Fig. 3c). The basal-level of H3K27me3 in the 7 h shade-induced genes was higher in *ref6-1* than in Col-0 based on GSE65329¹⁹ (Fig. 3d). This elevated H3K27me3 in *ref6-1* was much more pronounced on the *REF6*-bound 7 h shade-induced genes (Fig. 3e). Moreover, we obtained similar results using other published RNA-sequence datasets with 1 h (GSE210807¹⁶) and 6 h (GSE226205²⁰) shade treatments (Supplementary Fig. 3).

To verify and extend the above observation, we performed quantitative PCR analyses on some selected genes. Based on the overlap between *REF6*-bound genes and 7 h shade-induced genes, we chose to analyse *LNG2*, *EXPA11*, *XTH22* and *XTH23* in Col-0 and *ref6-1* at 1 h and 8 h of shade treatment. These genes have been reported to be involved in hypocotyl elongation and/or shade avoidance^{21–25}. Our RT-qPCR data revealed that in Col-0, the transcription levels of these genes were induced significantly at 8 h but not at 1 h of shade

treatment (Fig. 3f). In *ref6-1*, the expression levels of these genes were all reduced (Fig. 3f).

To investigate whether an increased H3K27me3 level could be associated with reduced expression levels of shade-induced genes in *ref6-1*, we carried out chromatin immunoprecipitation coupled with quantitative PCR analyses (ChIP-qPCR) with anti-H3K27me3 antibody. Our results showed that the H3K27me3 levels at *LNG2*, *EXPA11*, *XTH22* and *XTH23* did not change significantly upon shade treatment but were clearly increased in *ref6-1* under all the studied conditions (Fig. 3g). These results indicated that, although shade barely influences the level of H3K27me3, basal levels of H3K7me3 are indeed determinant for transcription levels of shade-induced genes.

The expressions of these late shade-induced genes correlated with growth defect of *ref6* in phase IV under N condition. However, this category of gene cannot explain the growth defect in phase II under P condition, indicating there may be an alternative regulatory mechanism.

Shade barely affects global genome-wide binding of REF6

The *REF6* gene itself was not responsive to shade, as evidenced by its relatively constant transcript and protein levels in our analyses (Supplementary Fig. 4a, b).

To test whether shade affects genome-wide binding of *REF6*, we performed ChIP-seq analysis using the *proREF6:REF6-HA/ref6-1* seedlings grown under N_WL and N_SH 8 h with an anti-HA antibody. A total of 7726 and 7205 peaks covering 7026 and 6702 genes (overlapping between two replicates, $FC > 2$ and $q < 0.05$) were bound by *REF6-HA* under N_WL and N_SH 8 h, respectively (Supplementary Data 4). These identified *REF6-HA*-bound genes were largely overlapped with the previously published *REF6-HA*-bound genes¹⁹ (Supplementary Fig. 4c). And the top enriched-motif bound by *REF6-HA* was CTCTGTTT, similar to that previously reported²⁶ (Supplementary Fig. 4d). Moreover, the results shown in Fig. 3a and Supplementary Fig. 3a were further supported by our data obtained under N_WL and N_SH 8 h, showing that there were more *REF6-HA*-bound genes associated with late than early shade-induced genes (Supplementary Fig. 4e, f). Remarkably, we found that the enrichment patterns of *REF6-HA* between N_WL and N_SH 8 h were highly correlated and overlapped with each other (Fig. 4a–c). We further examined the enrichment of *REF6-HA* at *LNG2*, *EXPA11*, *XTH22* and *XTH23*. Consistent with H3K27me3 profiles (Fig. 3g), the enrichments of *REF6-HA* were barely affected by shade treatment at these examined genes (Fig. 4d, e). Taken together, these results indicate that shade does not affect obvious global genome-wide binding of *REF6-HA*.

REF6 and PIF7 regulate the expression of shade-memory-related genes

If *REF6* participates in SAS only for maintaining the induction potential of shade-induced genes, the *REF6* loss-of-function mutant should display the same shade avoidance memory phenotype as Col-0 under P condition. However, both *ref6-1* and *ref6-3* showed defective memory phenotypes, and the growth rate patterns of *ref6-1* and *ref6-3* were different between the N and P conditions. This suggests that *REF6* has additional roles in shade avoidance memory.

According to the shade memory phenotype, plants acclimatized to shade respond to the triggering shade more strongly than non-acclimatized plants. Therefore, we conducted RNA sequencing to identify shade-memory-related genes whose inductions were enhanced in primed plants compared to naïve plants in response to triggering shade (Supplementary Fig. 5a). GO analysis of shade-induced genes, identified from both naïve and primed plants with the cut-offs $FC > 1.5$ and $P < 0.05$, indicated that “shade avoidance”, “response to auxin”, and “response to red or far-red light” are highly enriched terms (Supplementary Fig. 5a–c, Supplementary Data 5), which is consistent with previously published datasets^{15,27}.

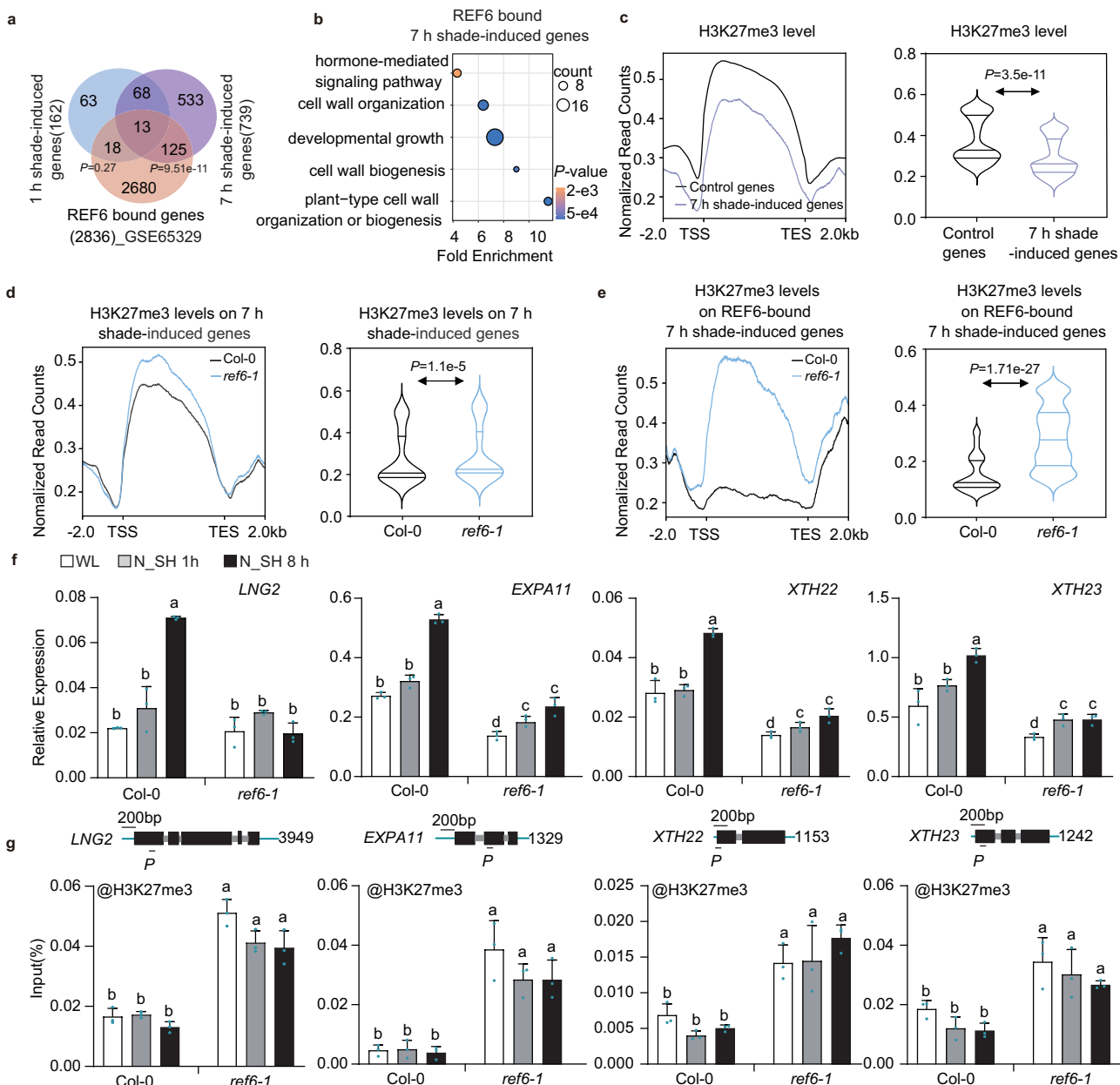


Fig. 3 | REF6 maintains low H3K27me3 levels on late shade-induced genes.

a Venn diagram showing the overlapping genes between 1 h and 7 h shade-induced genes and REF6 bound genes. The source data for shade-induced genes at 1 h and 7 h are from GSE59722. The source data for REF6 binding genes are from GSE65329. The *P* value was calculated by Fisher's exact test. **b** Gene Ontology (GO) analysis of REF6-bound 7 h shade-induced genes. For each point, the size is proportional to the number of genes, and the colours represent the *P* value, Fisher's one-tailed test. **c** Average density plot (left) and violin plot (right) showing the distribution profile of H3K27me3 levels on control genes (all non-induced genes by shade) and 7 h shade-induced genes. **d** Average density plot (left) and violin plot (right) showing the distribution profile of H3K27me3 levels of 7 h shade-induced genes in the Col-0 and *ref6-1*. **e** Average density plot (left) and violin plot (right) showing the distribution profile of H3K27me3 levels of REF6-bound 7 h shade-induced genes in

Col-0 and *ref6-1*. **f** Relative expression levels of *LNG2*, *EXP11*, *XTH22* and *XTH23* in Col-0 and *ref6-1*. **g** H3K27me3 enrichment on the *LNG2*, *EXP11*, *XTH22* and *XTH23* loci in Col-0 and *ref6-1*. The top panels show a schematic representation of the gene structures and the positions of primers. The bottom panels show the effects of shade on H3K27me3 enrichment. The enrichment of H3K27me3 was calculated as input%. In **c–e**, the source data are from GSE65329. The *P* value was calculated by Welch's *t*-test (two-sided). In **f** and **g**, seedlings that were grown under white light for 6 d and then maintained under white light or transferred to shade for 1 h and 8 h. Data are presented as mean values \pm SD ($n = 3$, where n refers to biological replicates). Different letters indicate statistically significant differences ($P < 0.05$) by one-way ANOVA with Tukey's HSD test. Source data are provided as a Source Data file.

The inductions of shade-induced genes identified in naïve plants were found reduced in both *pif7-1* and *ref6-1* under N condition, and the reductions were less severe under P condition (Supplementary Fig. 5d). Vice versa, the inductions of shade-induced genes identified in primed plants were reduced in both *pif7-1* and *ref6-1* more severely under P condition than N condition (Supplementary Fig. 5e). These results indicate that shade-induced genes were different between naïve and

primed plants, which contributed to the shade deficits under N condition and shade memory deficits under P condition, respectively.

Then, we chose genes with increased shade-induction (1478, $FC > 1.2$) under P compared to N conditions and referred them as shade-memory-related genes (Fig. 5a, Supplementary Data 6). The enriched growth-related GO terms (auxin-activated signalling pathway, growth, cell wall organization) in these shade-memory-related

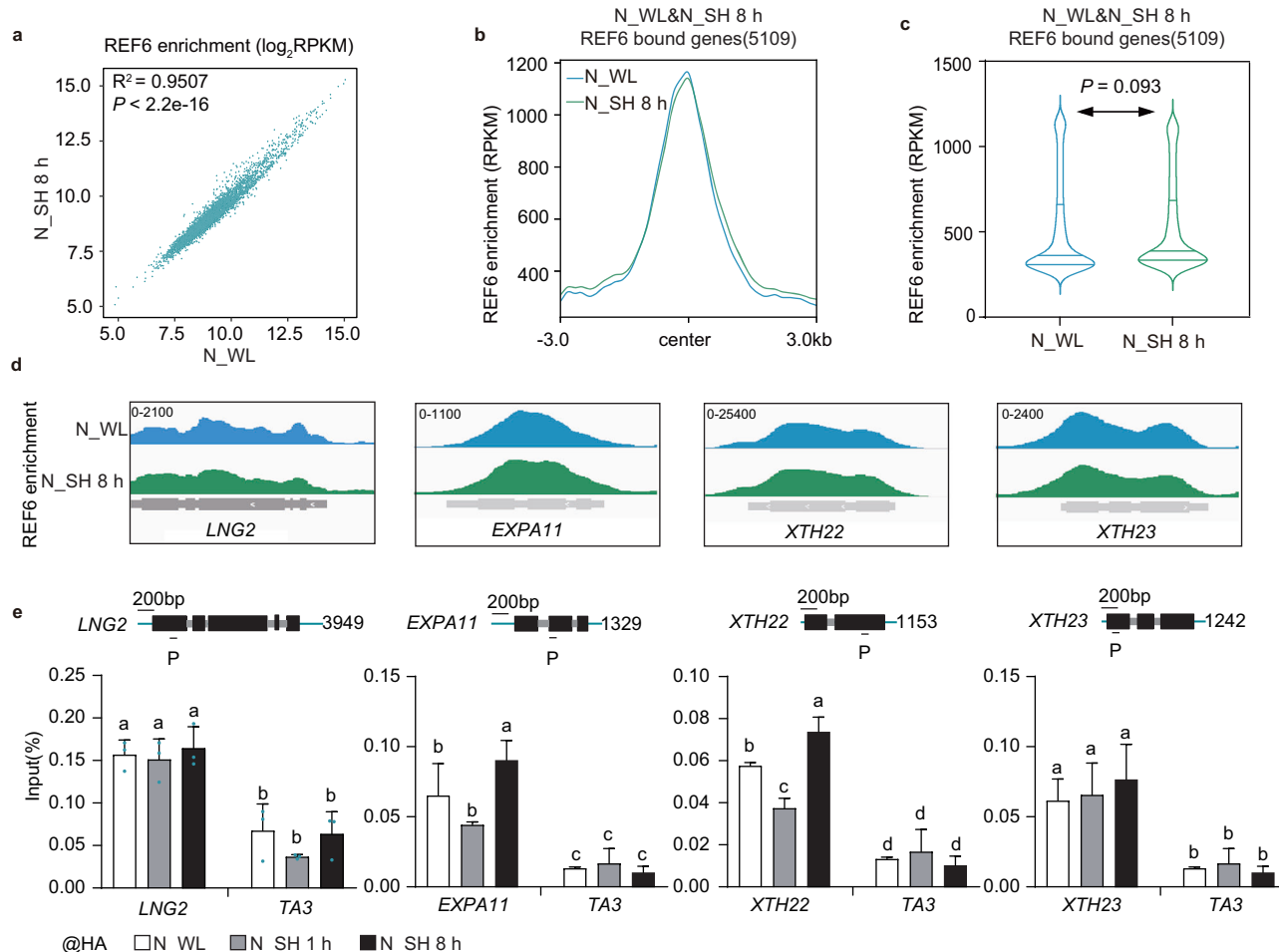


Fig. 4 | Shade barely affects global genome-wide binding of REF6. **a** Scatterplots of normalized REF6 ChIP-seq signal intensity in log₂ for overlap regions between the N_WL and N_SH 8 h conditions. The profiles were generated after merging two biological replicates. The *P* value was calculated by *t*-test (two-sided). Average density plot (**b**) and violin plot (**c**) displaying the REF6-HA enrichment on N_WL&N_SH 8 h REF6 bound genes (5109) under N_WL and N_SH 8 h conditions. The *P* value was calculated by Welch's *t*-test (two-sided). The profiles were generated after merging two biological replicates. **d** Representative genome browser view of REF6-HA binding to the LNG2, EXPA11, XTH22 and XTH23 loci in

proREF6::REF6-HA/ref6-1 under N_WL and N_SH 8 h conditions. **e** ChIP-qPCR analysis of REF6-HA enrichment using an anti-HA antibody at the LNG2, EXPA11, XTH22 and XTH23 loci in proREF6::REF6-HA/ref6-1. TA3 is a transposon and served as a negative control. The top panels show a schematic representation of the gene structures and positions of primers. REF6 enrichment was calculated as input%. Different letters indicate statistically significant differences ($P < 0.05$) based on one-way ANOVA with Tukey's HSD test. Data are presented as mean values \pm SD ($n = 3$, where n refers to technical replicates). Source data are provided as a Source Data file.

genes (Fig. 5b, Supplementary Data 7) supported the increased growth rates under P conditions. These results suggest that transcriptional memory²⁸ participates in shade avoidance memory.

Moreover, the shade induction of these shade-memory-related genes was impaired in primed *ref6-1* and more severely in primed *pif7-1* (Fig. 5a, c), which is consistent with the shade memory defective phenotypes of these mutants. To further explore whether the effect of REF6 on shade avoidance memory is associated with PIF7, we used mfuzz clustering of differentially expressed shade-memory-related genes in Col-0, *pif7-1* and *ref6-1*. An optimal number of clusters (four) were identified by using Pearson correlation based on levels of gene expression. We found two clusters (C1:401, C3:443 genes) (Supplementary Data 8) comprising 844 downregulated genes in both *pif7-1* and *ref6-1* (Fig. 5c), in which growth terms were enriched, such as cell wall organization, response to hormone, and growth. The previous examined genes LNG2, EXPA11, XTH22 and XTH23 were absent from this list of 844 genes. Interestingly, five other genes (IAA19, BGL1, GH3.6, PRE1 and YUCCA2) previously reported as playing a role on hypocotyl elongation and/or shade avoidance^{29–34} were among the identified genes. The triggering-shade induction of IAA19, BGL1, GH3.6, PRE1 and YUCCA2 in plants grown under N and P conditions were further

confirmed by RT-qPCR analysis (Fig. 5d and Supplementary Fig. 5f). The decreased triggering-shade induction of these genes in primed *pif7-1* and *ref6-1* as well as in primed *elf6-3* was also confirmed (Fig. 5d and Supplementary Fig. 5f–g). Together, these results establish that PIF7 and REF6/ELF6 participate in regulating the expression of shade-memory-related genes.

Demethylation of H3K27me3 at certain shade-memory-related genes is mediated by PIF7 and REF6

Next, we re-analysed our REF6-HA ChIP-seq data by specifically focusing on the 844 shade-memory-related genes coregulated by PIF7 and REF6. Interestingly, these genes showed a moderate but statistically significant higher enrichment of REF6-HA under N_SH 8 h than under N_WL conditions (Fig. 6a). To further explore REF6-HA binding at shade-memory-related genes, we identified shade-increased REF6-HA-binding genes by using lower FC (N_SH 8 h / N_WL > 1.2. Supplementary Data 9) and compared them with the 844 shade-memory-related genes and PIF7-bound genes (GSE156584³⁵). This led to the identification of 17 common genes and 17 shade-memory-related genes showing shade-increased enrichment of REF6-HA but not PIF7-bound (Fig. 6b). Growth-related GO terms were enriched mainly in the

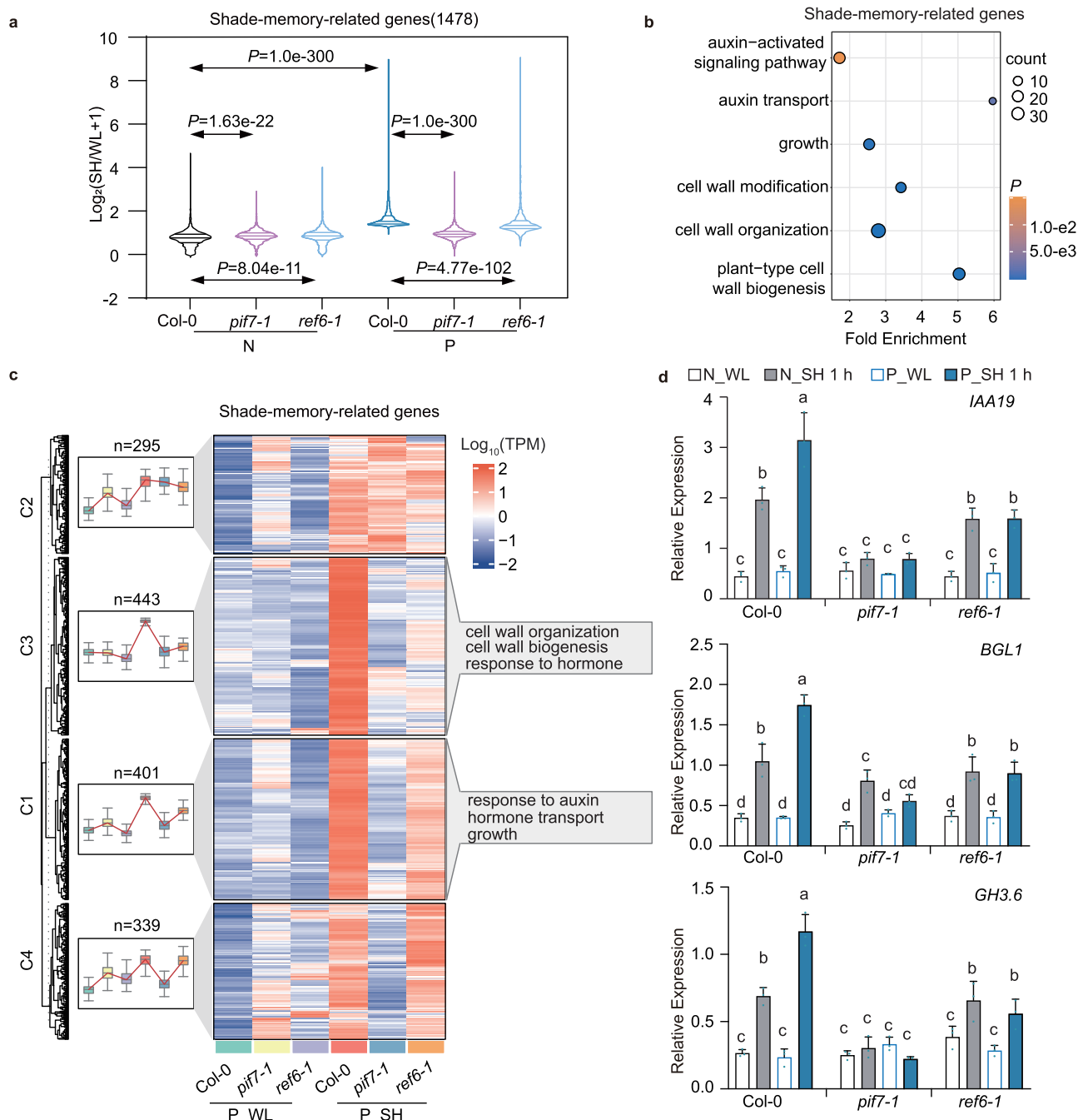


Fig. 5 | Transcriptome profiling reveals shade-memory-related genes. **a** Boxplot displaying the shade induction of shade-memory-related genes in *Col-0*, *pif7-1* and *ref6-1* under N and P conditions. The *P* value was calculated by the Mann-Whitney *U* test (two-sided). **b** Gene Ontology (GO) analysis of shade-memory-related genes. For each point, the size is proportional to the number of genes, and the colours represent the *P* value, Fisher's one-tailed test. **c** Mfuzz clustering of differentially expressed shade-memory-related genes in *Col-0*, *pif7-1* and *ref6-1*. Boxplots show the median (horizontal line), second to third quartiles (box), and whiskers extend to a maximum of 1.5× interquartile range beyond the box. GO analysis of genes in the C1 and C3 clusters are presented on the right side of heatmap. Orange and blue indicate RNA expression at high and low levels, respectively. **d** Relative expression levels of *IAA19*, *BGL1* and *GH3.6* in *Col-0*, *pif7-1* and *ref6-1* seedlings. The sampling conditions are shown in Supplementary Fig. 5a. Different letters indicate statistically significant differences (*P* < 0.05) based on one-way ANOVA with Tukey's HSD test. Data are presented as mean values \pm SD ($n = 3$, where n refers to biological replicates). Source data are provided as a Source Data file.

REF6 and PIF7 co-targeted genes (Fig. 6c). The shade-increased enrichment of REF6-HA was found greater for these REF6 and PIF7 co-targeted genes (Fig. 6d).

We were curious to know why the enrichment of REF6-HA increased on a number of PIF7-targeted genes under shade. First, we confirmed the binding of PIF7 at *IAA19*, *BGL1*, *GH3.6*, *PRE1* and *YUCCA2* by ChIP-qPCR analysis (Fig. 6e and Supplementary Fig. 6b–c). Then, we checked the H3K27me3 levels on PIF7-targeted genes in white light-grown naïve plants (N_WL), 1 h shade-treated naïve plants (N_SH 1 h), 8 h shade-treated naïve plants (N_SH 8 h), recovering primed plants (P_WL), and 1 h shade-treated primed plants (P_SH 1 h) (the treatment of samples was shown in Supplementary Fig. 6a). The transcriptional level of *PP2AA3* is not regulated by shade and is unchanged in *ref6-1* and *pif7-1* according to our qRT-PCR results (Supplementary Fig. 6d), and there is H3K27me3 mark at the *PP2AA3* locus based on the previously published

REF6 and PIF7 co-targeted genes (Fig. 6c). The shade-increased enrichment of REF6-HA was found greater for these REF6 and PIF7 co-targeted genes (Fig. 6d).

We were curious to know why the enrichment of REF6-HA increased on a number of PIF7-targeted genes under shade. First, we confirmed the binding of PIF7 at *IAA19*, *BGL1*, *GH3.6*, *PRE1* and *YUCCA2* by ChIP-qPCR analysis (Fig. 6e and Supplementary Fig. 6b–c). Then, we checked the H3K27me3 levels on PIF7-targeted

genes in white light-grown naïve plants (N_WL), 1 h shade-treated naïve plants (N_SH 1 h), 8 h shade-treated naïve plants (N_SH 8 h), recovering primed plants (P_WL), and 1 h shade-treated primed plants (P_SH 1 h) (the treatment of samples was shown in Supplementary Fig. 6a). The transcriptional level of *PP2AA3* is not regulated by shade and is unchanged in *ref6-1* and *pif7-1* according to our qRT-PCR results (Supplementary Fig. 6d), and there is H3K27me3 mark at the *PP2AA3* locus based on the previously published

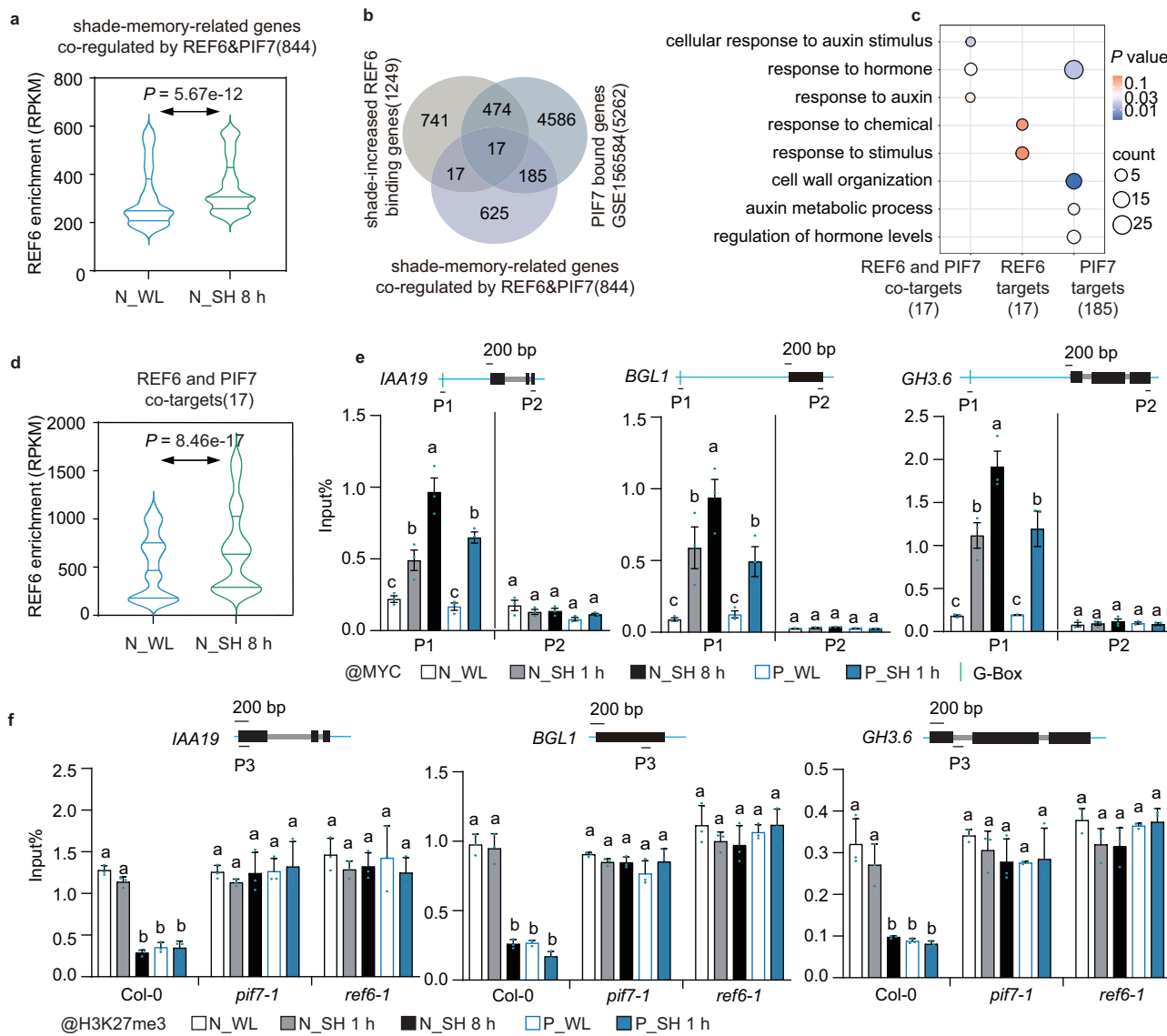


Fig. 6 | Demethylation of H3K27me3 at certain shade-memory-related genes is mediated by PIF7 and REF6. **a** Violin plot displaying the REF6 enrichment under N_WL and N_SH 8 h conditions on shade-memory-related genes co-regulated by REF6 and PIF7. **b** Venn diagram showing the overlapping genes between shade-increased REF6 binding genes (N_SH 8 h vs. N_WL > 1.2), PIF7 bound genes and shade-memory-related genes co-regulated by REF6 and PIF7. The source data for PIF7 bound genes were obtained from GSE156584. **c** Gene Ontology (GO) analysis of PIF7 targets (bound and regulated genes), PIF7 and REF6 cotargets (bound and regulated genes) and REF6 targets (bound and regulated genes) in shade-memory-related genes. For each point, the size is proportional to the number of genes, and the colours represent the *P* value, Fisher's one-tailed test. **d** Violin plot displaying the REF6 enrichment of REF6 and PIF7 co-targets under N_WL and N_SH 8 h.

e ChIP-qPCR analysis of PIF7 enrichment using an anti-MYC antibody at the *IAA19*, *GH3.6* and *BGL1* in 3S::PIF7-Flash. **f** ChIP-qPCR analysis of H3K27me3 enrichment using anti-H3K27me3 antibody at the *IAA19*, *GH3.6* and *BGL1* loci in Col-0, *pif7-1* and *ref6-1*. In **a** and **d**, the *P* value was calculated in a window from the 3 kb upstream REF6 binding summit to the 3 kb downstream by Welch's *t*-test (two-sided). In **e** and **f**, the sampling conditions are shown in Supplementary Fig. 6a. The top panels show a schematic representation of the gene structures and position of primer and enrichment was calculated as input%. Different letters indicate statistically significant differences (*P* < 0.05) based on one-way ANOVA with Tukey's HSD test. Data are presented as mean values \pm SD ($n = 3$, where n refers to biological replicates). Source data are provided as a Source Data file.

H3K27me3 ChIP-seq data (GSE18129³⁶). Therefore, we chose *PP2AA3* as a negative control for H3K27me3 in our ChIP-qPCR analysis. Remarkably, 1 h of shade did not change the level of H3K27me3 on our examined genes in either naïve or primed plants (N_WL vs. N_SH 1 h, P_WL vs. P_SH 1 h), but 8 h of shade decreased H3K27me3 levels (N_WL vs. N_SH 8 h). Low levels of H3K27me3 were maintained during the recovery time (P_WL) and 1 h of triggering shade time (P_SH 1 h) (Fig. 6f and Supplementary Fig. 6e). The level of H3K27me3 on *PP2AA3* was stable under all our tested conditions and in all our studied genotypes (Supplementary Fig. 6e). As expected, the reductions in H3K27me3 caused by 8 h of shade were absent in *pif7-1* and *ref6-1* (Fig. 6f), suggesting that both PIF7 and REF6 are

required for the observed changes of H3K27me3 at these examined shade-memory-related genes.

Enrichment of REF6 at certain shade-memory-related genes is dependent on PIF7

Next, we asked the question whether REF6 enrichment at shade-memory-related genes dependent on PIF7. For this, we investigated the enrichment of REF6-HA in the *pif7-1* background under N_SH 8 h by ChIP-seq analysis. A total of 5956 peaks covering 5687 genes were identified to be associated with REF6-HA binding in *pif7-1* (overlapping between two replicates, FC > 2 and *q* < 0.05, Supplementary Data 10). There were 4760 overlapped REF6-HA binding genes between *ref6-1*

and *pij7-1* background (Fig. 7a). The enrichment patterns of REF6-HA on these genes were highly correlated in *pij7-1* as compared to *ref6-1* (Fig. 7b–c). To further explore the effect of PIF7 on REF6-HA binding, we identified increased and decreased REF6-HA-binding genes in *pij7-1* by using FC > 1.2 (Supplementary Data 11). Growth related GO terms, such as response to light stimuli, response to hormone, were enriched in decreased REF6-HA-binding genes in *pij7-1* (Fig. 7d), in which there were 312 PIF7 bound genes (Fig. 7e). A reduction of REF6-HA enrichment in *pij7-1* as compared to *ref6-1* was observed on the REF6 and PIF7 co-targeted genes identified in Fig. 6b (Fig. 7f), suggesting a pivotal role of PIF7 in REF6 enrichment on certain shade-memory-related genes.

We further performed ChIP-qPCR analysis to verify the binding of REF6 at *IAA19*, *BGL1*, *GH3.6*, *PRE1* and *YUCCA2* in white light-grown naïve plants (N_WL), 1 h shade-treated naïve plants (N_SH 1 h), 8 h shade-treated naïve plants (N_SH 8 h), recovering primed plants (P_WL), and 1 h shade-treated primed plants (P_SH 1 h). We found that the enrichment of REF6-HA increased after 8 h of shade treatment (N_WL vs. N_SH 8 h) and this increase was maintained after 40 h recovering and 1 h of triggering shade (N_SH 8 h vs. P_WL and P_WL vs. P_SH 1 h) (Fig. 7g and Supplementary Fig. 7a). Interestingly, in *pij7-1*, the enrichment of REF6-HA remained low at all our studied treatment conditions (Fig. 7g and Supplementary Fig. 7a). Together with the ChIP-seq data, these ChIP-qPCR results support that the shade-induced enrichment of REF6 on certain shade-memory-related genes was dependent on PIF7.

Then we questioned whether the expression of *PIF7* and *REF6* disturbed each other. We analysed their transcript and/or protein level changes in *pij7-1* and *ref6-1* during the first and second light transitions. REF6 levels were quite stable and barely affected in *pij7-1* (Supplementary Fig. 7b–d). The transcript level of *PIF7* was repressed by shade in Col-0 as well as in *ref6-1* (Supplementary Fig. 7e). While dephosphorylated PIF7 accumulated with shade treatment (Supplementary Fig. 7f), which is consistent with previous reports^{8,37}. These results indicate that the expression of *PIF7* does not depend on the function of *REF6* and vice versa.

PIF7 binds REF6

Next, we tested the protein–protein interaction between PIF7 and REF6. We first used a luciferase complementation imaging (LCI) assay. As shown in Fig. 8a, nLUC-tagged PIF7 could interact with the cLUC-tagged C-terminus of REF6 when it was transiently expressed in *Nicotiana benthamiana* leaf cells. We successfully expressed SUMO-His-PIF7 and GST-REF6C, but failed to express GST-REF6 in *E. coli*. In an in vitro pull-down assay, SUMO-His-PIF7 proteins purified from *E. coli* were bound by GST-REF6C proteins purified from *E. coli* but not GST alone (Fig. 8b). To further examine the interaction between REF6 and PIF7 in vivo, we crossed the *proREF6::REF6-HA/ref6-1* line with the *35S::PIF7-Flash* (9 × Myc-6 × His-3 × Flag) line and performed co-immunoprecipitation (Co-IP) assays. As shown in Fig. 8c, the dephosphorylated, but not the phosphorylated, PIF7-Flash extracted from *proREF6::REF6-HA/ref6-1* *35S::PIF7-Flash* could be precipitated by REF6-HA using an HA antibody. Since the dephosphorylated PIF7 protein accumulated with shade treatment, we further explored the interaction strength of REF6 and PIF7 over the time course of shade treatment. As expected, we found that more REF6-HA formed protein complexes with cumulative dephosphorylated PIF7-Flash (Fig. 8d). This finding suggests that PIF7 recruited more REF6 to participate in the removal of H3K27me3 on shade-memory-related genes during 8 h of priming shade treatment.

Because the C-terminus of REF6 is highly homologous with that of ELF6 (Supplementary Fig. 8a), we also verified and confirmed the interaction between PIF7 and the C-terminus of ELF6 in LCI and in vitro GST pull-down assays (Supplementary Fig. 8b, c).

We further analysed the genetic relationship between PIF7 and REF6/ELF6 in shade memory determinacy. The primed shade-induced hypocotyl elongation disappeared in the double mutants *pij7-1ref6-1*, *pij7-1ref6-3* and *pij7-1elf6-3*, which behaved more like *pij7-1* (Fig. 8e, and Supplementary Fig. 8d). Growth rate measurements confirmed that the *pij7-1ref6-1*, *pij7-1ref6-3* and *pij7-1elf6-3* mutants displayed shade avoidance memory defects resembling those of *pij7-1* (Fig. 2a, Fig. 8f, Supplementary Fig. 8e). These results suggest that PIF7 and REF6/ELF6 are required for shade avoidance memory.

Taken together, our results suggest that under prolonged shade, accumulated PIF7 can recruit REF6/ELF6, which reduces the level of H3K27me3 in shade-memory-related genes (Fig. 8g). These genes become more inclined to be induced in primed plants than in naïve plants, contributing to faster hypocotyl elongation under recurring shade (Fig. 8g).

Discussion

In nature, environmental changes, particularly stressful abiotic conditions, are often chronic or recurring. The initial response may be different from the long-term response and may prime a plant to respond differently to recurrence of the same condition. Although shade is not an extreme or harmful stress, plants have evolved sophisticated ways to acclimate or adjust their growth patterns according to the environmental conditions¹. Shade-intolerant plants, such as *Arabidopsis*, are able to quickly change gene expression programmes within minutes after the onset of shade conditions¹². With time, the transcriptional response diverges²⁷. Most gene expression changes can be reversed after the seedlings are returned to white light. The distinct expression patterns were observed between naïve and primed plants under the same triggering condition. These altered gene expression responses that occur upon repeated exposure to a condition have been termed transcriptional memory^{38–41}.

In the current study, we identified shade induced transcriptional memory. The H3K27me3 mark negatively regulates gene expression⁴² and a low level of H3K27me3 is a prerequisite for shade induction by *LNG2*, *EXPA11*, *XTH22* and *XTH23* (Fig. 3). Our work indicates that REF6 is responsible for maintaining the potential of certain REF6-targeted genes to be induced by shade. A similar mechanism was also reported under warm temperatures³⁶. Prolonged shade-induced genes include more REF6-targeted genes, which explains why the effect of REF6 on hypocotyl elongation mainly occurred at the late stage (Phase IV) under N condition (Fig. 2b, Supplementary Fig. 4g).

Meanwhile, shade led to a significant decrease in H3K27me3 levels in *PRE1*, *YUCCA2*, *IAA19*, *BGL1* and *GH3.6*, accompanied by increased enrichment of REF6 after 8 h of priming shade treatment (Fig. 6). In addition to self-targeting, REF6 can be recruited to PIF7's targets (Figs. 7, 8). These genes maintain lower levels of H3K27me3 during recovery compared to those in a plant in the naïve state. Although these changes are PIF7 dependent, PIF7 dissociates from these loci during recovery. A low level of H3K27me3 is retained to mediate transcriptional memory in the absence of ongoing transcription. When primed plants face shade again, the induction of these genes becomes stronger and occurs earlier (Fig. 8g).

Together, the results of our study reveal the molecular mechanism by which REF6 participates in the transcriptional response to prolonged shade and recurring shade and highlight the importance of the cooperation of epigenetic factors and transcription factors in regulating gene expression and environmental responses.

Within the same generation, the effects of priming can be maintained /remembered for a few days or weeks, suggesting that information can be stored during priming. This somatic transcriptional memory has been reported for drought response, salt response, development and differentiation, and so on. For example, the $\Delta 1$ -pyrroline-5-carboxylate synthetase 1 (P5CS1) gene shows transcriptional memory (enhanced reinduction) in response to salt stress.

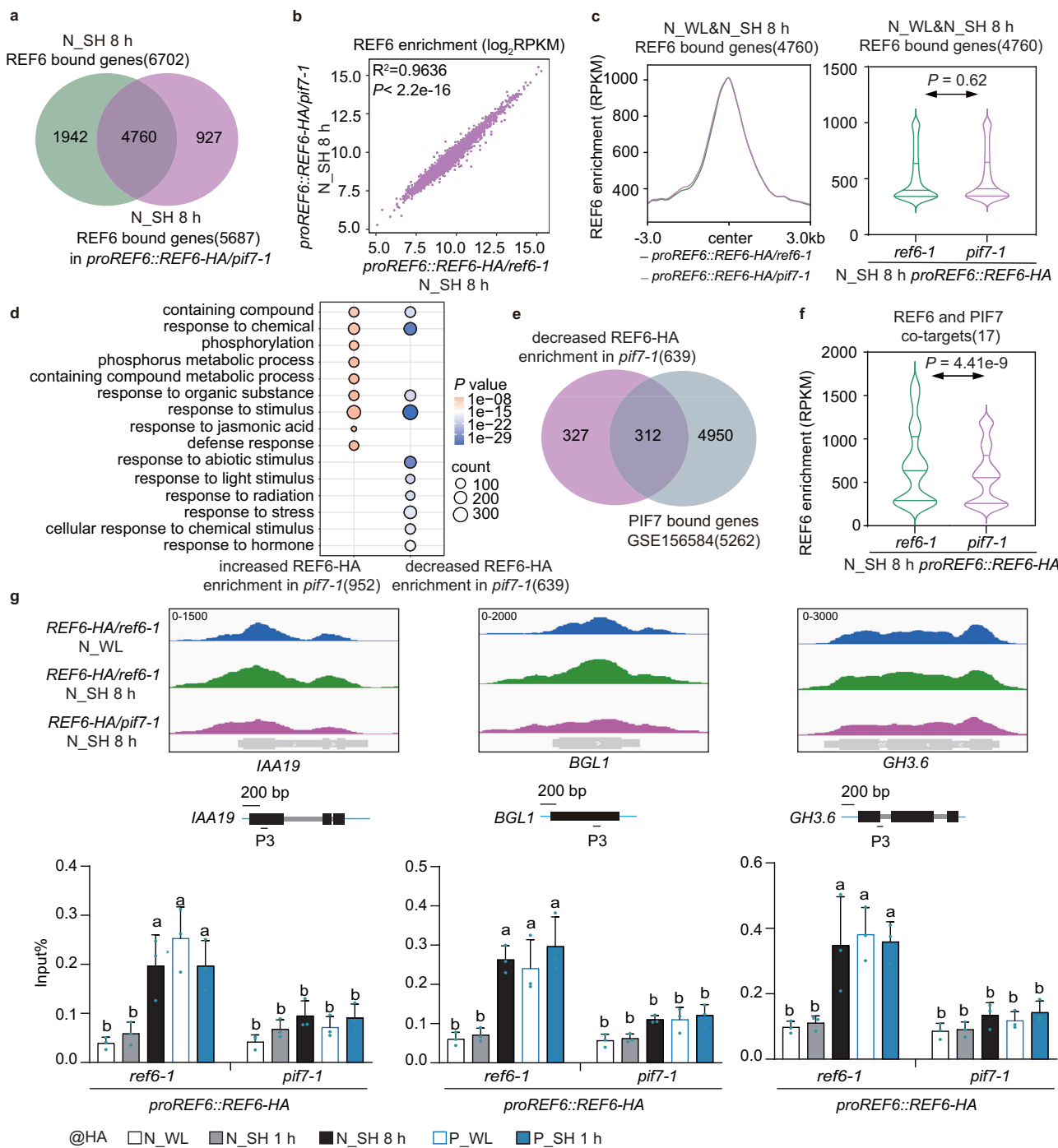


Fig. 7 | Enrichment of REF6 at certain shade-memory-related genes is dependent on PIF7. **a** Venn diagram showing the overlapping genes between N_SH 8 h REF6 bound genes and N_SH 8 h REF6 bound genes in *proREF6::REF6-HA/pif7-1*. The profiles were generated after merging two biological replicates. **b** Scatterplots of normalized REF6 ChIP-seq signal intensity in \log_2 scale of REF6 bound genes (4760) in *proREF6::REF6-HA/ref6-1* and *proREF6::REF6-HA/pif7-1* under N_SH 8 h conditions. The profiles were generated after merging two biological replicates. The P value was calculated by *t*-test (two-sided). **c** Average density plot (left) and violin plot (right) displaying the REF6-HA enrichment of REF6 bound genes (4760) in *proREF6::REF6-HA/ref6-1* and *proREF6::REF6-HA/pif7-1* under N_SH 8 h condition. The profiles were generated after merging two biological replicates. **d** Gene Ontology (GO) analysis of increased and decreased N_SH 8 h REF6 bound genes of *proREF6::REF6-HA/pif7-1* vs. *proREF6::REF6-HA/ref6-1* ($FC > 1.2$). For each point, the size is proportional to the number of genes, and the colours represent the P value, Fisher's one-tailed test. **e** Venn diagram showing the overlapping genes between

decreased REF6 bound genes in *proREF6::REF6-HA/pif7-1*, PIF7 bound genes and shade-memory-related genes co-regulated by REF6 and PIF7. **f** Violin plot displaying the REF6-HA enrichment of REF6 and PIF7 co-targets (17) in *proREF6::REF6-HA/ref6-1* and *proREF6::REF6-HA/pif7-1* under N_SH 8 h condition. **g** ChIP-qPCR analysis of REF6-HA enrichment using an anti-HA antibody at the *IAA19*, *BGL1*, and *GH3.6* loci in *proREF6::REF6-HA/ref6-1* and *proREF6::REF6-HA/pif7-1*. The sampling conditions are shown in Supplementary Fig. 6a. The top panels show a IGV screenshots of REF6 binding peaks and the gene structure schematic of *IAA19*, *BGL1* and *GH3.6*. REF6 enrichment was calculated as input%. Different letters indicate statistically significant differences ($P < 0.05$) based on one-way ANOVA with Tukey's HSD test. Data are presented as mean values \pm SD ($n = 3$, where n refers to biological replicates). In **c** and **f**, the P value was calculated in a window from the 3 kb upstream REF6 binding summit to the 3 kb downstream by Welch's *t*-test (two-sided). Source data are provided as a Source Data file.

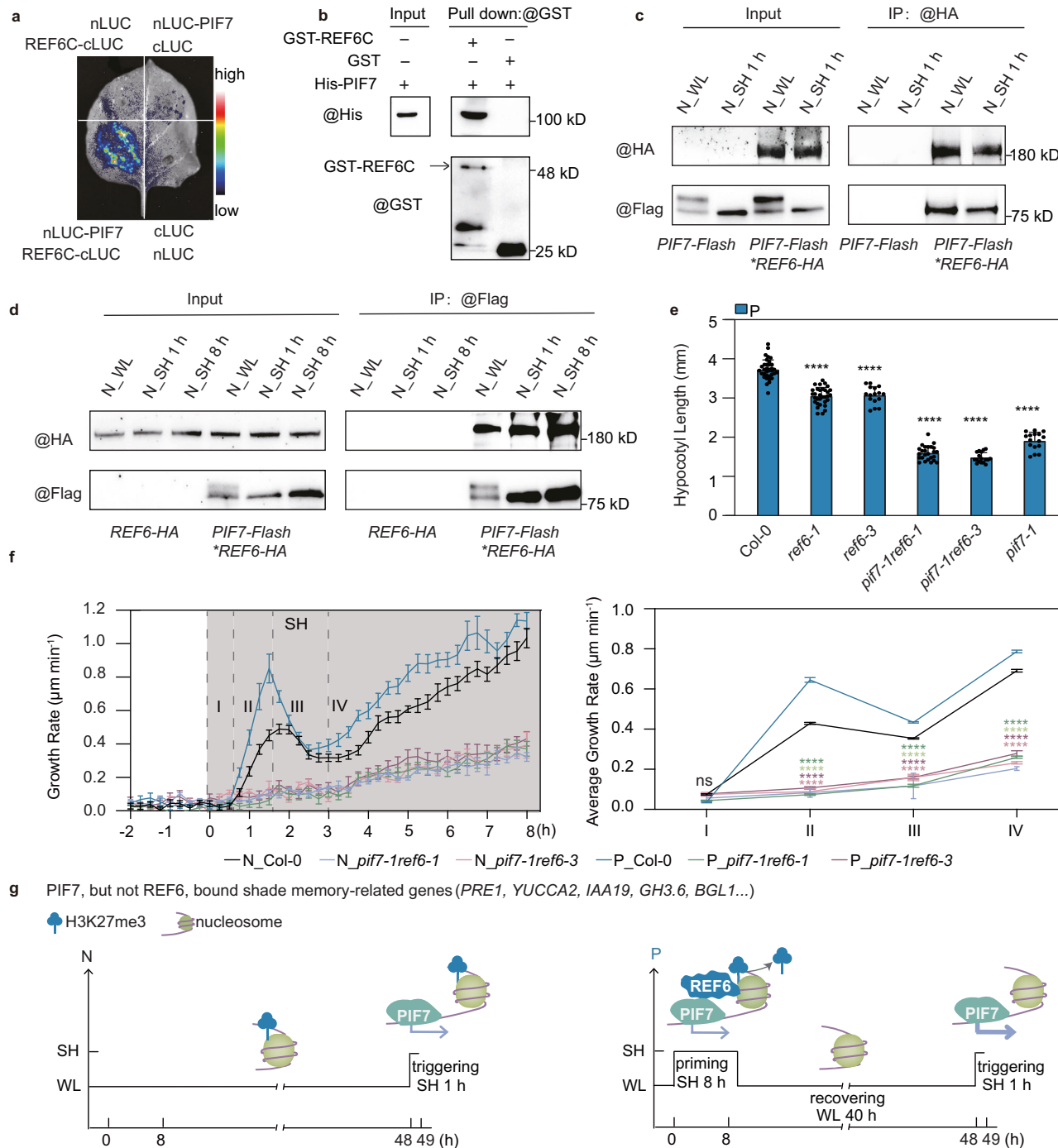


Fig. 8 | PIF7 physically interacts with REF6 to contribute to shade avoidance memory. **a** Interaction between PIF7 and the REF6C-terminal as detected by a luciferase complementation imaging (LCI) assay in *Nicotiana benthamiana*. **b** Interaction between PIF7 and the REF6C-terminal as detected by an in vitro GST pull-down assay. TF-His-fused PIF7 and GST-REF6C-terminal were purified from *E. coli*. **c** Interaction between PIF7 and REF6 in *Arabidopsis* as detected by an in vivo Co-IP assay. Anti-HA beads were used to precipitate REF6-HA from *proREF6:REF6-HA/ref6-1*35S:PIF7-Flash* seedlings grown under *N_WL* and *N_SH1h*. PIF7 and REF6 were detected by anti-Flag and anti-HA antibodies. **d** Shade effects on the interactions between PIF7 and REF6 in *Arabidopsis* was examined by Co-IP assays. Anti-Flag beads were used to precipitate PIF7-Flash from *proREF6:REF6-HA/ref6-1*35S:PIF7-Flash* seedlings grown under *N_WL*, *N_SH1h* and *N_SH8h*. PIF7 and REF6 were detected by anti-Flag and anti-HA antibodies. **e** Hypocotyl lengths of Col-0, *ref7-1ref6-1* and *ref7-1ref6-3* grown under P conditions which are shown in supplementary Fig. 1d. **f** Shade-triggered growth rates and average growth

rates of Col-0, *ref7-1ref6-1* and *ref7-1ref6-3* seedlings under N and P conditions. **g** Proposed working model of the PIF7 and REF6 during shade-avoidance memory. Under white light, the chromatin of certain shade-memory-related genes carry repressive histone modifications (H3K27me3) that inhibit spontaneous transcription. After 8 h priming shade, the accumulated PIF7 recruits REF6 to demethylate H3K27me3 and activates these certain shade-memory-related genes (e.g., *PRE1*, *YUCCA2*, *IAA19*, *GH3.6* and *BGL1*). During recovering white light condition, the expression levels of these certain shade-memory-related genes returned to normal levels in white light, but low levels of H3K27me3 were primed on these genes. When shade reoccurs, PIF7 quickly activates their expressions. In **e** and **f**, data are presented as mean values \pm SD (**e**) and SE (**f**) and the *P* value was calculated by One-way ANOVA with Tukey's HSD test (**e**) and Student's two-sided *t*-test (**f**), respectively, and significant differences are shown by ***(*P* < 0.0001). Source data are provided as a Source Data file.

Several epigenetic modifications have been implicated in stress memory after priming, such as histone H3K4 hypermethylation, histone H3K27 methylation, and nucleosome occupancy^{39,43}. The maintenance of a high level of H3K4me3 and stalled Ser5P RNA Polymerase II (Ser5P Po II) at stress memory genes helps plants remember experienced dehydration stress⁴⁴. Heat acclimation induces sustained H3K27me3 demethylation at *HEAT SHOCK PROTEIN22 (HSP22)* and *HSP17.6 C* loci, poising the *HSP* genes for subsequent activation⁴⁵. In mouse TT2 embryonic stem cells (ESCs), CpG island (CGI)-binding protein BEND3 is required for association with Polycomb repressive complex 2 (PRC2) at bivalent genes, playing a reining function in maintaining high levels of H3K27me3 at those bivalent genes in ESCs to prevent their premature activation in the forthcoming developmental stage⁴⁶. In fact, 36 years ago, persistent effects of longer periods of shade or FR treatment on elongation growth were first reported after the plants were returned to white light⁴⁷. Later, we have learned more about the link between photoreceptor excitation and changes in plant architecture, especially in hypocotyl elongation, in *Arabidopsis*. A longer duration of shade triggers more downstream events. In the present study, we identified H3K27me3 modifications and found that PIF7 and REF6 are involved in shade-induced transcriptional memory. Epigenetic changes occur during prolonged shade treatment and trigger extension growth when the seedlings are facing shade again. Whether and how other epigenetic mechanisms are linked to shade-induced transcriptional memory will be an interesting topic for further study.

The removal of H3K27me3 is catalysed by JmjC domain-containing histone demethylases, including in REF6, ELF6 and JUMONJI 13 (JMJ13)^{48–50}. A previous report suggested that REF6 and ELF6 are necessary for heat acclimation⁴⁵. Both the *ref6* and *elf6* single mutants displayed similar shade memory defects in terms of growth rate and hypocotyl length (Figs. 1g, 2a), while JMJ13-defective mutant displayed no such defects (Supplementary Fig. 2d). The *ref6-1elf6-3* showed slightly enhanced shade memory defects in hypocotyl length, suggesting that REF6 and ELF6 are partially redundant in shade memory. Due to their conserved C-terminus, both REF6 and ELF6 can be recruited by PIF7 (Fig. 8a–d and Supplementary Fig. 8) to certain shade- memory-related genes and regulate their expression in response to recurring shade (Supplementary Fig. 5g). This finding is comparable to a previous report showing that BES1 recruits REF6 and ELF6 to regulate target gene expression and coordinate the BR response⁵¹. It has also been reported that REF6 and ELF6 regulate the removal of H3K27me3 at different genomic loci due to their preference for binding motifs, which is supported by the distinct roles of REF6 and ELF6 in the maintenance of plant genome integrity⁵². However, due to the conserved motif, PIF7 can recruit both REF6 and ELF6, which have partially redundant functions in the response to recurring shade. The detailed features of this redundancy and differences among these three enzymes warrant more research.

Plants can remember past environmental conditions to better prepare for recurring stress⁵³. The duration of the memory varies depending on the type of environmental exposure. Here, we found that shade-induced memories are short-term memories. The effect of priming shade decreased with the extension of recovery time (Supplementary Fig. 1b). The length of the priming shade required for memory is related to the speed of H3K27me3 removal by demethylases. The recovery time may be dependent on the speed of writing of H3K27me3 and other epigenetic modifications. Heat induces transmitted phenotypes via a coordinated epigenetic network involving histone demethylases, transcription factors, and tasiRNAs, ensuring reproductive success and transgenerational stress adaptation⁵⁴. How the memory of shade is established and transmitted to progeny and whether phenotypes are affected remain largely unknown. These studies will further elucidate the mechanisms of plant adaptation and memory.

Methods

Plant materials and growth conditions

All *Arabidopsis* (*Arabidopsis thaliana*) plants used were in the Col-0 background. The information of mutants used in this study have been previously described: *pij7-1*⁸, *ref6-1*⁵⁵, *ref6-3*⁵⁵, *elf6-3*⁵⁵, *ref6-1elf6-3*⁵⁵, *proREF6::REF6-HA/ref6-1*⁵⁵, *clf28*, *sdg25-1*⁵⁶, *atx1-2*⁵⁶, *atx1-2sdg25-1*⁵⁶, *sdg8*, *jmj13g*³⁶, *phyB-9* and *35S::PIF7-Flash*⁸. The double mutants *pij7-1ref6-1*, *pij7-1ref6-3*, *pij7-1elf6-3*, *phyB-9ref6-1*, *phyB-9elf6-3* *proREF6::REF6-HA/pij7-1* and *proREF6::REF6-HA/ref6-1*35S::PIF7-Flash* were generated by genetic crossing and verified using phenotypic inspection, PCR genotyping, and/or sequencing.

For phenotypic analysis, seeds were germinated on plates containing 1/2 MS medium with 1% agar (Sangon, Shanghai, China) and without sucrose. After 5 days stratification, the plates were incubated in growth chambers under continuous white light (R, ~30 μ mol m⁻² s⁻¹; B, ~20 μ mol m⁻² s⁻¹; FR, ~8 μ mol m⁻² s⁻¹) and then transferred to shade (R, ~30 μ mol m⁻² s⁻¹; B, ~20 μ mol m⁻² s⁻¹; FR, ~65 μ mol m⁻² s⁻¹) at 22 °C. *Nicotiana benthamiana* plants were grown at 26 °C under long-day conditions with 16 h of light.

Hypocotyl measurement

The kinetics of hypocotyl growth were measured by a commercial high-throughput imaging platform, DynaPlant® (Microlens Technology, Beijing, <http://www.dynaplant.cn/en>). Seedlings for kinetic measurements were sown on 1/2 MS medium containing 2% phytigel (Solarbio, P8170) and grown under N (4-day-old seedlings + 8 h white light + 40 h recovering white light + 8 h triggering shade) and P (4-day-old seedlings + 8 h priming shade + 40 h recovering white light + 8 h triggering shade) conditions. The images of hypocotyl growth were captured by the DynaPlant® platform once every 15 min for each seedling with a physical resolution of 1.2 μ m per pixel. The lengths of new hypocotyl growth in the time-series images were quantified by DynaPlant Analysis software, which was provided by the instrument manufacturer. The values shown indicate the means with SEM.

Quantitative measurements of hypocotyl lengths were performed on scanned images of seedlings using ImageJ software. At least 16 seedlings were used per treatment or genotype.

RNA-seq analysis

For Fig. 3a, differential expression analysis was performed using DESeq2 with $|log_2\text{foldchange}| > \log_2(2)$ and $\text{FDR} < 0.05$ using a web-based tool (<http://bioinformatics.sdbstate.edu/idep/>). The raw RNA-seq data were obtained from GSE59722. For Fig. 5, seedlings were grown under N (4-day-old seedlings + 8 h white light + 40 h recovering white light + 1 h triggering shade) and P (4-day-old seedlings + 8 h priming shade + 40 h recovering white light + 1 h triggering shade) conditions. Two biological replicates were prepared for each genotype of the plants grown under light and shade conditions. Total RNA was extracted from snap-frozen tissues using TRIzol reagent according to the manufacturer's instructions (Invitrogen). RNA libraries were constructed and sequenced using Majorbio (<http://www.majorbio.com>). Differential expression analysis was performed using DESeq2 with $|log_2\text{foldchange}| > \log_2(1.5)$ and $P < 0.05$. The heatmap of shade memory-related genes was generated by gene expression pattern clustering analysis using Majorbio (<http://www.majorbio.com>). We chose genes with increased shade-induction ($FC > 1.2$) under P compared to N conditions in 1876 P_shade-induced genes and referred them as shade-memory-related genes. GO term enrichment analysis was conducted by the web-based tool DAVID.

Quantitative RT-PCR analysis

Approximately 100 mg of seedlings grown on 1/2 MS medium supplemented with 1% agar under different light conditions was collected in tubes, frozen in liquid nitrogen, and ground to a fine powder. Three biological replicates were prepared for each genotype of the plants

grown under white light and shade conditions (N, 4-day-old seedlings + 8 h white light + 40 h recovering white light + 1 h triggering shade; P, 4-day-old seedlings + 8 h priming shade + 40 h recovering white light + 1 h triggering shade). Total RNA was extracted using a TRIzol kit (Promega, USA). Two micrograms of total RNA were reverse transcribed using a First Strand cDNA Synthesis Kit (TIANGEN, China) according to the manufacturer's instructions. The cDNAs were then subjected to real-time qPCR using a CFX Connect Real-Time System (Bio-Rad, USA) and SYBR Green qPCR Mix (Mei5 Biochem, China). Three biological replicates per sample were used for the qRT-PCR analysis. The data are presented as the means with the SD of three biological replicates normalized to the expression of the reference gene *AT2G39960*. The comparative $\Delta\Delta Ct$ method was used to evaluate the relative quantities of each amplified product in the samples. The specificity of the qRT-PCRs was determined by melt curve analysis of the amplified products using the standard method. The primers used are listed in Supplementary Data 12.

ChIP-qPCR assay

For H3K27me3 ChIP-qPCR, Col-0, *pif7-1*, and *ref6-1* seedlings were grown under white light and shade conditions (N, 4-day-old seedlings + 8 h white light + 40 h white light + 1 h and 8 h triggering shade; P, 4-day-old seedlings + 8 h priming shade + 40 h white light + 1 h and 8 h triggering shade). Three biological replicates were prepared for each genotype of plants grown under light and shade conditions. For HA ChIP-qPCR, *proREF6::REF6-HA/ref6-1* and *proREF6::REF6-HA/pif7-1* seedlings were grown under white light and shade conditions (N, 4-day-old seedlings + 8 h white light + 40 h white light + 1 h and 8 h triggering shade; P, 4-day-old seedlings + 8 h priming shade + 40 h white light + 1 h triggering shade). Three biological replicates were prepared for each genotype of the plants grown under light and shade conditions. The seedlings were harvested and cross-linked for 15 min under vacuum in cross-linking buffer (extraction buffer 1 with 1% formaldehyde). Cross-linking was terminated with 125 mM glycine (pH 8.0) under vacuum for 5 min, and the seedlings were washed three times in double-distilled water and rapidly frozen. A bioruptor was used at high power with 15 30 s on /30 s off cycles until the average chromatin size was approximately 200-500 bp, followed by immunoprecipitation with an anti-HA (Lumiprobe sc-7392 X) or anti-H3K27me3 antibody (Millipore 07-449). RT-qPCR was performed using a kit from Takara to determine the enrichment of immunoprecipitated DNA in the ChIP experiments. The *TA3* retrotransposon (*AT1G37110*) and *AT2G39960* were used as the negative control region for ChIP-qPCR. The values in the graphs are the mean \pm SD. At least three independent biological replicates were performed. Statistical significance was determined by one-way ANOVA with Tukey's HSD test for multiple-pair comparisons. The primers used are listed in Supplementary Data 12.

ChIP-seq analysis

For REF6-HA binding ChIP, *proREF6::REF6-HA/ref6-1* (N_WL and N_SH 8 h) and *proREF6::REF6-HA/pif7-1* (N_SH 8 h) seedlings were prepared for each genotype of plants grown under white light and shade conditions (N, 4-day-old seedlings + 8 h white light + 40 h white light + 8 h triggering shade) using an anti-HA antibody (Lumiprobe sc-7392 X). The sample library was sequenced on a NovaSeq6000 PE150 by Shanghai Jiayin Biotechnology Ltd. A quality distribution plot and base content distribution were generated using FASTQC. Before read mapping, clean reads were obtained from the raw reads by removing adaptor sequences. The clean reads were aligned to the reference genome sequences using the BWA programme. The bam file was generated using the unique mapped reads as an input file, and using macs3 software for call peak with cutoff fold change > 2.0 and $q < 0.05$. The HOMER's findMotifsGenome.pl tool was used for Motif analysis. The input file is the peak file and the genome fasta file. The DNA

sequence is extracted according to the peak file, and the sequence is compared with the Motif database to obtain the Motif. DAVID was used to identify gene ontology enrichment in the ChIP-seq data. Visualization was performed with IGV version 2.7.2. Heatmaps and ChIP-seq profiles were generated using deepTools utilities plotHeatmap and plotProfile.

Firefly luciferase complementation imaging assays

The fragments encoding PIF7 were amplified by PCR and ligated into a pCAMBIA2300-nLUC vector to produce nLUC-PIF7. The coding regions of *REF6C-terminal* (3538-4083 bp) or *ELF6C-terminal* (3439-4023 bp) were amplified by PCR and ligated into pCAMBIA2300-cLUC to produce REF6C-cLUC or ELF6C-cLUC. The resulting constructs were transformed into *Agrobacterium* strain GV3101. *Agrobacterium* cells harbouring different constructs were then infiltrated into *N. benthamiana* leaves. Three days after infiltration, luciferin (Promega, USA) (2.5 mM, 0.1% Triton X-100) was spread before LUC activity was monitored by a Tanon 5500 chemical luminescence imaging system (Tanon, China).

Protein pull-down assay

The full-length *PIF7* CDS was cloned and inserted into pCold-His-TF (Takara, Beijing, China). The plasmid was transformed into *Escherichia coli* strain Rosetta (DE3), and protein production was induced by incubation in 200 mL of LB medium containing 0.5 mM IPTG at 16 °C for 16 h. The His-TF-PIF7 protein was bound to Ni NTA Beads 6FF (Smart-Lifesciences, SA005025) by incubation for approximately 2 h at 4 °C. In the GST pull-down assay, the TF-His-PIF7 protein was incubated with pretreated GST-REF6C or GST-ELF6C beads for 2 h. GST was used as the negative control. The beads were resuspended in SDS-PAGE loading buffer and analysed by SDS-PAGE and immunoblotting using the anti-His antibody.

Co-IP assay

Total protein extracts were prepared from *proREF6::REF6-HA/ref6-1*PIF7-Flash* seedlings grown under white light for 7 d and then treated with shade for 1 h or 8 h or maintained under white light. Anti-HA beads or anti-Flag beads were used to precipitate REF6-HA or PIF7-Flash from *proREF6::REF6-HA/ref6-1*PIF7-Flash* seedlings. PIF7-Flash and REF6-HA were detected by anti-Flag and anti-HA antibodies.

Statistics & reproducibility

All values are presented as means \pm SEM or SD and differences for which $P < 0.05$ were considered significant. Significance levels were defined as n.s. (not significant, $P > 0.05$), $^*P < 0.05$, $^{**}P < 0.01$, $^{***}P < 0.001$, and $^{****}P < 0.0001$. The number (n) of samples for each value is indicated in source data. Unless otherwise indicated, significant differences between the two samples were analysed with a two-tailed Student's *t*-test as indicated in figure legends. Significant differences for multiple comparisons were determined by one-way ANOVA with Tukey's HSD test as indicated in figure legends. Each experiment was repeated independently at least two times with consistent results.

Antibody information

The following antibodies were purchased: anti-Myc antibody (GNI, GNI4410-MC, 1:4000); anti-Flag antibody (GNI, GNI4410-FG, 1:1000); anti- β -Tubulin antibody (Abmart, M30109M, 1:4000); anti-GST antibody (Abmart, M20007, 1:4000); anti-His antibody (GNI, GNI4110-HS, 1:4000); anti-H3K27me3 antibody (Millipore 07-449, 1:1000); Anti-HA antibody (Lumiprobe sc-7392 X, 1:800); Glutathione Resin (GenScript, L00206); rProtein A Beads 4FF (Smart-Lifesciences, SA015005); Ni NTA Beads 6FF (Smart-Lifesciences, SA005025); Anti-DYKDDDDK Affinity Beads (Smart-Lifesciences, SA042100); Anti-HA Affinity Beads (Smart-Lifesciences, SA068100).

Reporting summary

Further information on research design is available in the Nature Portfolio Reporting Summary linked to this article.

Data availability

RNA-seq and ChIP-seq data have been deposited in the NCBI GEO database with accession number [GSE226745](https://doi.org/10.3390/gse226745) and [GSE268785](https://doi.org/10.3390/gse268785). Source data are provided with this paper.

References

1. Casal, J. J. Shade avoidance. *Arabidopsis Book* **10**, e0157 (2012).
2. Ballare, C. L. & Pierik, R. The shade-avoidance syndrome: multiple signals and ecological consequences. *Plant Cell Environ.* **40**, 2530–2543 (2017).
3. Cerdan, P. D. & Chory, J. Regulation of flowering time by light quality. *Nature* **423**, 881–885 (2003).
4. Izaguirre, M. M., Mazza, C. A., Biondini, M., Baldwin, I. T. & Ballare, C. L. Remote sensing of future competitors: impacts on plant defenses. *Proc. Natl. Acad. Sci. USA* **103**, 7170–7174 (2006).
5. Schmitt, J., Dudley, S. A. & Pigliucci, M. Manipulative approaches to testing adaptive plasticity: phytochrome-mediated shade-avoidance responses in plants. *Am. Nat.* **154**, S43–S54 (1999).
6. Leivar, P. & Quail, P. H. PIFs: pivotal components in a cellular signaling hub. *Trends Plant Sci.* **16**, 19–28 (2011).
7. Burko, Y. et al. PIF7 is a master regulator of thermomorphogenesis in shade. *Nat. Commun.* **13**, 4942 (2022).
8. Li, L. et al. Linking photoreceptor excitation to changes in plant architecture. *Genes. Dev.* **26**, 785–790 (2012).
9. Willige, B. C. et al. PHYTOCHROME-INTERACTING FACTORs trigger environmentally responsive chromatin dynamics in plants. *Nat. Genet.* **53**, 955–961 (2021).
10. Cole, B., Kay, S. A. & Chory, J. Automated analysis of hypocotyl growth dynamics during shade avoidance in *Arabidopsis*. *Plant J.* **65**, 991–1000 (2011).
11. Hwang, Y. S. & Quail, P. H. Phytochrome-regulated PIL1 derepression is developmentally modulated. *Plant Cell Physiol.* **49**, 501–511 (2008).
12. Salter, M. G., Franklin, K. A. & Whitelam, G. C. Gating of the rapid shade-avoidance response by the circadian clock in plants. *Nature* **426**, 680–683 (2003).
13. Peng, M. et al. Linking PHYTOCHROME-INTERACTING FACTOR to histone modification in plant shade avoidance. *Plant Physiol.* **176**, 1341–1351 (2018).
14. Nguyen, N. H. et al. HISTONE DEACETYLASE 9 promotes hypocotyl-specific auxin response under shade. *Plant J.* <https://doi.org/10.1111/tpj.16410> (2023).
15. Yang, C. et al. PIF7-mediated epigenetic reprogramming promotes the transcriptional response to shade in *Arabidopsis*. *EMBO J.* **42**, e111472 (2023).
16. Zhu, T., Yang, C., Xie, Y., Huang, S. & Li, L. Shade-induced lncRNA PUAR promotes shade response by repressing PHYA expression. *EMBO Rep.* **24**, e56105 (2023).
17. Harris, C. J., Amtmann, A. & Ton, J. Epigenetic processes in plant stress priming: open questions and new approaches. *Curr. Opin. Plant Biol.* **75**, 102432 (2023).
18. Huang, S., Yang, C. & Li, L. Unraveling the dynamic integration of auxin, brassinosteroid and gibberellin in early shade-induced hypocotyl elongation. *Phenomics* **2**, 119–129 (2022).
19. Cui, X. et al. REF6 recognizes a specific DNA sequence to demethylate H3K27me3 and regulate organ boundary formation in *Arabidopsis*. *Nat. Genet.* **48**, 694–699 (2016).
20. Huang, S. et al. Shade-induced RTFL/DVL peptides negatively regulate the shade response by directly interacting with BSKs in *Arabidopsis*. *Nat. Commun.* **14**, 6898 (2023).
21. Hwang, G. et al. PIF4 promotes expression of LNG1 and LNG2 to induce thermomorphogenic growth in *Arabidopsis*. *Front Plant Sci.* **8**, 1320 (2017).
22. Song, B. et al. Phytochrome A inhibits shade avoidance responses under strong shade through repressing the brassinosteroid pathway in *Arabidopsis*. *Plant J.* **104**, 1520–1534 (2020).
23. Guo, H. et al. Three related receptor-like kinases are required for optimal cell elongation in *Arabidopsis thaliana*. *Proc. Natl. Acad. Sci. USA* **106**, 7648–7653 (2009).
24. Claisse, G., Charrier, B. & Kreis, M. The *Arabidopsis thaliana* GSK3/Shaggy like kinase AtSK3-2 modulates floral cell expansion. *Plant Mol. Biol.* **64**, 113–124 (2007).
25. Polko, J. K. et al. Ethylene-induced differential petiole growth in *Arabidopsis thaliana* involves local microtubule reorientation and cell expansion. *N. Phytol.* **193**, 339–348 (2012).
26. Qiu, Q. et al. DNA methylation repels targeting of *Arabidopsis* REF6. *Nat. Commun.* **10**, 2063 (2019).
27. Kohnen, M. V. et al. Neighbor detection induces organ-specific transcriptomes, revealing patterns underlying hypocotyl-specific growth. *Plant Cell* **28**, 2889–2904 (2016).
28. D'Urso, A. & Brickner, J. H. Mechanisms of epigenetic memory. *Trends Genet.* **30**, 230–236 (2014).
29. Zhou, X. Y., Song, L. & Xue, H. W. Brassinosteroids regulate the differential growth of *Arabidopsis* hypocotyls through auxin signaling components IAA19 and ARF7. *Mol. Plant* **6**, 887–904 (2013).
30. Nakazawa, M. et al. DFL1, an auxin-responsive GH3 gene homologue, negatively regulates shoot cell elongation and lateral root formation, and positively regulates the light response of hypocotyl length. *Plant J.* **25**, 213–221 (2001).
31. Ikeda, M., Fujiwara, S., Mitsuda, N. & Ohme-Takagi, M. A triantagonistic basic helix-loop-helix system regulates cell elongation in *Arabidopsis*. *Plant Cell* **24**, 4483–4497 (2012).
32. Nozue, K. et al. Shade avoidance components and pathways in adult plants revealed by phenotypic profiling. *PLoS Genet.* **11**, e1004953 (2015).
33. Lee, S. et al. Overexpression of PRE1 and its homologous genes activates Gibberellin-dependent responses in *Arabidopsis thaliana*. *Plant Cell Physiol.* **47**, 591–600 (2006).
34. Staswick, P. E. et al. Characterization of an *Arabidopsis* enzyme family that conjugates amino acids to indole-3-acetic acid. *Plant Cell* **17**, 616–627 (2005).
35. Yang, C. et al. Two bHLH transcription factors, bHLH48 and bHLH60, associate with phytochrome interacting factor 7 to regulate hypocotyl elongation in *Arabidopsis*. *Cell Rep.* **35**, 109054 (2021).
36. He, K. et al. The histone H3K27 demethylase REF6/JMJ12 promotes thermomorphogenesis in *Arabidopsis*. *Natl. Sci. Rev.* **9**, nwab213 (2022).
37. Huang, X. et al. Shade-induced nuclear localization of PIF7 is regulated by phosphorylation and 14-3-3 proteins in *Arabidopsis*. *Elife* **7**, <https://doi.org/10.7554/elife.31636> (2018).
38. Zhao, Z. et al. Sustained TNF-alpha stimulation leads to transcriptional memory that greatly enhances signal sensitivity and robustness. *Elife* **9**, <https://doi.org/10.7554/elife.61965> (2020).
39. Oberkofer, V., Pratz, L. & Baurle, I. Epigenetic regulation of abiotic stress memory: maintaining the good things while they last. *Curr. Opin. Plant Biol.* **61**, 102007 (2021).
40. Lamke, J. & Baurle, I. Epigenetic and chromatin-based mechanisms in environmental stress adaptation and stress memory in plants. *Genome Biol.* **18**, 124 (2017).
41. Conrath, U., Beckers, G. J., Langenbach, C. J. & Jaskiewicz, M. R. Priming for enhanced defense. *Annu. Rev. Phytopathol.* **53**, 97–119 (2015).

42. Hugues, A., Jacobs, C. S. & Roudier, F. Mitotic inheritance of PRC2-mediated silencing: mechanistic insights and developmental perspectives. *Front. Plant Sci.* **11**, 262 (2020).
43. Baurle, I. Can't remember to forget you: chromatin-based priming of somatic stress responses. *Semin. Cell Dev. Biol.* **83**, 133–139 (2018).
44. Avramova, Z. Transcriptional 'memory' of a stress: transient chromatin and memory (epigenetic) marks at stress-response genes. *Plant J. Cell Mol. Biol.* **83**, 149–159 (2015).
45. Yamaguchi, N. et al. H3K27me3 demethylases alter HSP22 and HSP17.6C expression in response to recurring heat in *Arabidopsis*. *Nat. Commun.* **12**, 3480 (2021).
46. Zhang, J. J. et al. Highly enriched BEND3 prevents the premature activation of bivalent genes during differentiation. *Science* **375**, 1053–1058 (2022).
47. Casal, J. J. & Smith, H. Persistent effects of changes in phytochrome status on internode growth in light-grown mustard: Occurrence, kinetics and locus of perception. *Planta* **175**, 214–220 (1988).
48. Lu, F., Cui, X., Zhang, S., Jenuwein, T. & Cao, X. *Arabidopsis* REF6 is a histone H3 lysine 27 demethylase. *Nat. Genet.* **43**, 715–719 (2011).
49. Yan, W. et al. Dynamic and spatial restriction of Polycomb activity by plant histone demethylases. *Nat. Plants* **4**, 681–689 (2018).
50. Zheng, S. et al. The *Arabidopsis* H3K27me3 demethylase JUMONJI 13 is a temperature and photoperiod dependent flowering repressor. *Nat. Commun.* **10**, 1303 (2019).
51. Yu, X. et al. Modulation of brassinosteroid-regulated gene expression by Jumonji domain-containing proteins ELF6 and REF6 in *Arabidopsis*. *Proc. Natl. Acad. Sci. USA* **105**, 7618–7623 (2008).
52. Antunez-Sanchez, J. et al. A new role for histone demethylases in the maintenance of plant genome integrity. *Elife* **9**, <https://doi.org/10.7554/elife.58533> (2020).
53. Crisp, P. A., Ganguly, D., Eichten, S. R., Borevitz, J. O. & Pogson, B. J. Reconsidering plant memory: Intersections between stress recovery, RNA turnover, and epigenetics. *Sci. Adv.* **2**, e1501340 (2016).
54. Liu, J. et al. An H3K27me3 demethylase-HSFA2 regulatory loop orchestrates transgenerational thermomemory in *Arabidopsis*. *Cell Res.* **29**, 379–390 (2019).
55. Wang, X. et al. REF6 promotes lateral root formation through de-repression of PIN1/3/7 genes. *J. Integr. Plant Biol.* **61**, 383–387 (2019).
56. Song, Z. T., Zhang, L. L., Han, J. J., Zhou, M. & Liu, J. X. Histone H3K4 methyltransferases SDG25 and ATX1 maintain heat-stress gene expression during recovery in *Arabidopsis*. *Plant J. Cell Mol. Biol.* **105**, 1326–1338 (2021).

Acknowledgements

We are grateful to Prof. Guodong Ren (Fudan University) for sharing *ref6-1*, *ref6-3*, *elff6-3*, *ref6-1elff6-3*, *proREF6::REF6-HA/ref6-1* and *clf28*, Prof. Jianxiang Liu (Zhejiang University) for sharing *atx1-2*, *sdg25-1* and *atx1-sdg25* mutants, and Prof. Xiaofeng Cao (Institute of Genetics and Devel-

opmental Biology, Chinese Academy of Sciences) for sharing the seeds of *jmj13g*. This research was supported by funding provided by the National Natural Science Foundation of China to L.L. (NSFC32030018), and W.-H.S. received support from the Centre National de la Recherche Scientifique (Laboratoire International Associé Plant Epigenetic Research) and the Agence National de la Recherche (ANR-19-CE20-0018).

Author contributions

L.L. designed the experiments; Q.C. performed most of the experiments with the assistance from Y.Z., S.H., C.Y., and Y.X.; Q.C., L.L. and W.-H.S. analysed the data; L.L. wrote the manuscript and revised the manuscript with W.-H.S.

Competing interests

The authors declare no competing interests.

Additional information

Supplementary information The online version contains supplementary material available at <https://doi.org/10.1038/s41467-024-51834-4>.

Correspondence and requests for materials should be addressed to Lin Li.

Peer review information *Nature Communications* thanks Jorge Casal, and the other, anonymous, reviewer(s) for their contribution to the peer review of this work. A peer review file is available.

Reprints and permissions information is available at <http://www.nature.com/reprints>

Publisher's note Springer Nature remains neutral with regard to jurisdictional claims in published maps and institutional affiliations.

Open Access This article is licensed under a Creative Commons Attribution-NonCommercial-NoDerivatives 4.0 International License, which permits any non-commercial use, sharing, distribution and reproduction in any medium or format, as long as you give appropriate credit to the original author(s) and the source, provide a link to the Creative Commons licence, and indicate if you modified the licensed material. You do not have permission under this licence to share adapted material derived from this article or parts of it. The images or other third party material in this article are included in the article's Creative Commons licence, unless indicated otherwise in a credit line to the material. If material is not included in the article's Creative Commons licence and your intended use is not permitted by statutory regulation or exceeds the permitted use, you will need to obtain permission directly from the copyright holder. To view a copy of this licence, visit <http://creativecommons.org/licenses/by-nc-nd/4.0/>.

© The Author(s) 2024